NASA TECHNICAL
MEMORANDUM

NASA TM X-64592

SHUTTLE SIMULATION

By Alberta King and Maurice Knighton
Aero-Astrodynamics Laboratory

May 10, 1971

NASA

George C. Marshall Space Flight Center
Marshall Space Flight Center, Alabama

1. Report No.	2. Government Accession No.	3. Recipient's Catalog No.
NASA TM X-64592		

4. Title and Subtitle	5. Report Date
SHUTTLE SIMULATION	May 10, 1971
	6. Performing Organization Code

7. Author(s)	8. Performing Organization Report No.
Alberta King and Maurice Knighton	
	10. Work Unit No.

9. Performing Organization Name and Address	11. Contract or Grant No.
George C. Marshall Space Flight Center Marshall Space Flight Center, Alabama 35812	
	13. Type of Report and Period Covered

12. Sponsoring Agency Name and Address	13. Type of Report and Period Covered
	TECHNICAL MEMORANDUM
NASA Washington, D. C. 20546	14. Sponsoring Agency Code

15. Supplementary Notes

16. Abstract

The unique concepts of the Space Shuttle and the varied environments of its typical missions require a different analysis approach from previous launch vehicles. This becomes apparent when the reusability concept is analyzed. Since man will generally be on board, maximum utilization of his adaptive capabilities is highly desirable.

To properly analyze the interactions of man, machine, and environment, and to have the capability of analyzing automatic guidance and control concepts, a special simulation tool is required. The purpose of this report is to present the present simulation concept under development at MSFC, its capabilities, and future development plans. Included also are the 6-D equations of motion in modular form so that simulation of the various concepts (control) can be made easily. Detailed descriptions of the cockpit and visual displays are shown.

17. Key Words (Suggested by Author(s))	18. Distribution Statement
Shuttle Simulation Man-Machine Landing GN&C Displays	Unclassified - unlimited E. D. Geissler Director-Aero-Astrodynamics Laboratory

19. Security Classif. (of this report)	20. Security Classif. (of this page)	21. No. of Pages	22. Price*
UNCLASSIFIED	UNCLASSIFIED	72	$3.00

*For sale by the Clearinghouse for Federal Scientific and Technical Information
Springfield, Virginia 22151

TABLE OF CONTENTS

LIST OF ILLUSTRATIONS

LIST OF ILLUSTRATIONS (Continued)

DEFINITION OF SYMBOLS

Symbol	Definition
m	aircraft mass
U,V,W	components of total aircraft velocity, $\|V_p\|$ along the x,y,z body axes
F_x,F_y,F_z	components of the total external forces (including power plant, aerodynamic and gravity forces) along the x,y,z body axes
I_{xx},I_{yy},I_{zz}	moments of inertia about the x,y,z body axes
I_{xz}	product of inertia between the x and z body axes
P,Q,R	components of total aircraft angular velocity along the x,y,z body axes
M_x,M_y,M_z	components of total external moment (including powerplant and aerodynamic moments) along the x,y,z body axes
P_x,P_y,P_z	powerplant forces along the x,y,z axes
X,Y,Z	aerodynamic forces (including control-surface forces) along the x,y,z axes
T_x,T_y,T_z	powerplant moments along the x,y,z axes (T_x = 0 for turbojets and rockets)
L,M,N	aerodynamic moments (including control-surface effects) along the x,y,z axes
$\dot{S}_x$	velocity north
$\dot{S}_y$	velocity east
$-\dot{S}_z$	rate of climb
V_{WXB}	wind component in x direction (body axis)

V_{WYB}	wind component in y direction (body axis)
V_{WZB}	wind component in z direction (body axis)
X_s, Y_s, Z_s	aerodynamic forces along the x_s, y_s, z_s stability axes
L_s, M_s, N_s	aerodynamic moments along the x_s, y_s, z_s stability axes
S	wing area
b	wing span
c	characteristic wing chord
$C_{\mathscr{D}}, C_Y, C_{\mathscr{L}}$	dimensionless aerodynamics force coefficients along the stability axes
C_L, C_M, C_N	dimensionless aerodynamic moment coefficients along the stability axes ($L = \ell$ in most literature)
ρ	air density
β	angle of sideslip
α	angle of attack
δ_a	aileron displacement
δ_e	elevator displacement
δ_r	rudder displacement
P_s, Q_s, R_s	component of total aircraft angular velocity along the x_s, y_s, z_s stability axes
ψ	heading angle
θ	attitude angle
Φ	bank angle
g	gravity
V_p	vehicle velocity
K_γ	commanded glide path

H_1	commanded altitude for initial flare
h_2	commanded altitude for final flare
K_f	constant gain
η_{zc}	commanded g (load) level
$\delta_{sa}, \delta_{se}, \delta_{sr}$	stick commands for aileron, elevator and rudder
$\bar{P}$	roll rate
$\bar{Q}$	pitch rate
$\bar{R}$	yaw rate
S_c	desired altitude
$\dot{S}_c$	desired altitude rate
ψ_c	desired heading angle
θ_c	desired attitude angle
P_x, P_y, P_z	powerplant forces along the x,y,z body axes (P_y is normally zero)
S_y	heading
δ_t	percent of throttle
δ_{trim}	throttle trim
V_D	desired velocity
t	time
τ_D	lag in thrust
P_{xj}	thrust for each engine in x direction
R_{it}	thrust from each reaction jet
$\lambda_x, \lambda_y, \lambda_z$	orientation of reaction jet engines off the body axes so the thrust is lined up with the body axes

F_{irx}	forward force due to reaction jets
F_{iry}	lateral forces due to reaction jets
F_{irz}	normal force due to reaction jets
L_{R_i}	roll moment due to reaction jets
M_{R_i}	pitch moment due to reaction jets
N_{R_i}	yaw moment due to reaction jets
k_1, k_2	gains
γ	glide slope angle
$P_{J_{max}}$	maximum thrust
τ_a	time delay on aileron control
τ_e	time delay on elevator control
τ_r	time delay on rudder control
X_{cg}	location of the center of gravity in the x direction
Y_{cg}	location of the center of gravity in the y direction
Z_{cg}	location of the center of gravity in the z direction
C_o	aerodynamic force coefficient at zero lift
C_q	drag coefficient due to pitch rate
C_i	induced drag
$C_{Y\beta}$	aerodynamic side force coefficient due to sideslip angle
C_{Yr}	aerodynamic side force coefficient due to yaw rate

C_{Yp}	aerodynamic side force coefficient due to roll rate
$C_{Y\delta_r}$	aerodynamic side force coefficient due to rudder deflection
$C_{Y\dot{\beta}}$	aerodynamic side force coefficient due to sideslip rate
C_{Yo}	aerodynamic side force coefficient at zero sideslip
C_{α}	lift coefficient due to angle of attack
C_{δ_e}	lift coefficient due to elevator deflection
C_{q}	lift coefficient due to pitch rate
C_{o}	lift coefficient at zero angle of attack
$C_{L\beta}$	rolling moment coefficient due to sideslip angle
C_{Lp}	rolling moment coefficient due to roll rate
C_{Lr}	rolling moment coefficient due to yaw rate
$C_{L\delta_a}$	rolling moment coefficient due to aileron deflection
C_{Lo}	rolling moment coefficient at zero sideslip
$C_{M\alpha}$	pitching moment coefficient due to angle of attack
C_{Mq}	pitching moment coefficient due to pitch rate
$C_{M\dot{\alpha}}$	pitching moment coefficient due to angle of attack rate
$C_{M\delta_e}$	pitching moment coefficient due to elevator deflection
C_{Mo}	pitching moment coefficient at zero angle of attack
$C_{N\beta}$	yawing moment coefficient due to sideslip angle

C_{Nr}	yawing moment coefficient due to yaw rate
$C_{N\delta_r}$	yawing moment coefficient due to rudder deflection
C_{No}	yawing moment coefficient for zero sideslip
a_{a_o}	position gain on the aileron
a_{a_1}	rate gain on the aileron
g_o	path control gain on heading error
g_1	path control gain on heading rate error
a_{a_2}	path control gain on heading error
a_{e_o}	position error on attitude error on elevator
a_{e_1}	gain on pitch rate error on elevator
h_o	path control on altitude error
h_1	path control on altitude rate error
a_{r_2}	position gain on rudder
a_{r_3}	rate gain on rudder
a_{r_o}	gain on path angle rate
a_{r_1}	gain on roll rate

SHUTTLE SIMULATION

SUMMARY

The unique concepts of the Space Shuttle and the varied environments of its typical missions require a different analysis approach from previous launch vehicles. This becomes apparent when the reuseability concept is analyzed. Since man will generally be on board, maximum utilization of his adaptive capabilities is highly desirable.

To properly analyze the interactions of man, machine, and environment, and to have the capability of analyzing automatic guidance and control concepts, a special simulation tool is required. The purpose of this report is to present the present simulation concept under development at MSFC, its capabilities, and future development plans. Included also are the 6-D equations of motion in modular form so that simulation of the various concepts (control) can be made easily. Detailed descriptions of the cockpit and visual displays are shown.

I. INTRODUCTION

The Space Shuttle vehicle, as now envisioned, is sensitive to payload and fatigue (i.e., it is to be reuseable), and requires a highly integrated avionics system to meet the total mission requirements. The complexity of the mission is indicated on Figure 1 showing a typical mission profile.

The varied vehicle and environment characteristics associated with liftoff, ascent, separation, docking, orbit, deorbit, reentry, cruise, and landing phases are included in the mission. Analyses of these phases from the dynamics and control standpoint are very complicated using conventional automatic control logic. When the requirement of manual takeover for each phase is included, the analysis and design problem becomes even more complex. Not only must the system perform satisfactorily in the automatic mode, but it must also meet handling specifications in the manual mode.

Analysis and design of the control system and the prediction of the dynamic characteristics (response and loads), of necessity, require a good simulation. For the Shuttle vehicle, this means an accurate representation of the vehicle dynamics, the environment (atmospheric,

thermal, runway, etc.), the control system, and man. Analytical models can usually be adequately formulated for everything except man, who must be active instead of simulated. This means that the system (simulation) must provide both visual and motion cues for proper evaluation of the man and the machine. Since the Shuttle mission is so varied, only the reentry, cruise, and landing are included in this paper, although the cockpit portion will be applicable to all phases and can be connected to the ascent hybrid computer simulation if desired. This hybrid program for the ascent phase is being developed separately.

The key to the utility of a simulation is flexibility, simplicity, and low cost, which were the overriding considerations in developing the present program. Several aspects were taken into consideration:

1. The dynamic portion of the simulation must be applicable to reentry, cruise and landing studies and the cockpit must be applicable to all phases of the flight.

2. The simulation can be run with or without cockpit and visual displays for manual and automatic control, and for analysis of handling qualities.

3. Basic subsystems are programmed in modular form to allow flexibility in making changes, incorporating new concepts, etc.

4. The final dynamic simulation will be on the hybrid computer to facilitate time-varying and nonlinear data considerations.

5. The simulation will be capable of taking input disturbances, such as winds and ground proximity.

This paper presents the present simulation at MSFC, including cockpit and displays under development with pertinent equations, definitions, and future plans.

The describing equations of motion are 6-D with a capability of handling nonlinear aerodynamics. The use of Euler angles in the conventional aircraft form allows for a complete 6.28 rad turn maneuver with full roll capability, but the vehicle cannot fly a full 1.57 rad straight up or down because of the so-called gimbal lock. The equations are implemented modularly such that guidance and control concepts can be quickly changed.

This report is a joint effort of Aero-Astrodynamics Laboratory and the Computation Laboratory, Marshall Space Flight Center.

Many thanks are due to the programmer Barry Gregory and to William McClendon, who implemented the cockpit equipment. Without their excellent cooperation, the project could not have been done.

II. EQUATIONS OF MOTION

The increasing importance of being able to solve the nonlinear flight equations on high speed computers and in real time is obvious in the design of the autopilot, the control system, and the guidance system, and in the general field of flight simulation where the pilot or hardware is included in the control loop. The equations are developed with this goal in mind.

If the Shuttle vehicle is considered to be a rigid body in space, six degrees of freedom are necessary to describe its motion, translation and rotation along the x,y, and z axes. The orthogonal right-hand set of coordinates attached to the vehicle with the origin at the vehicle center of gravity is known as the body-axis system. The x and z axes lie in the plane of symmetry of the vehicle. The x axis is in the longitudinal direction of the craft, positive x toward the nose. The y axis lies perpendicular to the x axis with the positive direction to the right of the positive x direction. The positive z direction is toward the bottom of the craft (Figure 2).

The translational velocity components, denoted by U, V, and W, lie along the x,y,z body axes, respectively. The rotational components are P, Q, and R along the respective x, y, and z axes.

To completely determine the motion of the Shuttle vehicle, it is necessary to calculate the forces and moments acting on the vehicle resulting from gravity, inertia, power plant thrust and aerodynamic forces and moments.

To calculate the gravity forces, it is necessary to compute the orientation of the vehicle with respect to the earth axes. These calculations can be made by use of Euler angles or by direction cosines. Although this simulation used the Euler angle method, other approaches could be easily incorporated. Euler angles refer to attitude, bank, and heading angles (Figure 3).

The attitude angle, θ, is measured in the vertical plane containing the x axis and is the angle between the horizontal plane and the x axis; θ is positive for a climbing vehicle and varies between $\pm \pi/2$.

The bank angle, Φ, is the angle between the horizontal plane and the y axis. Looking at the vehicle from tail to nose, when the left wing is up and the right wing is down, Φ is positive.

The heading angle, ψ, is measured in the horizontal plane and is the angle between due north and the projection of the x axis on the horizontal plane. All of these angles are fed into the cockpit instrumentation and autopilot system.

Besides being used to compute the gravity forces for the translational equations, the Euler angles are necessary to compute the velocities $\dot{S}_x$ (velocity north), $\dot{S}_y$ (velocity east), and $-\dot{S}_z$ (rate of climb) along the earth axes.

The forces F_x, F_y, and F_z are made up of the sum of powerplant, aerodynamic, and gravity forces; whereas, the moments M_x, M_y, and M_z are made up of only the sum of powerplant and aerodynamic moments. The gravity moments are zero since the origin of the body axis is at the center of gravity of the vehicle. The aerodynamic forces and moments are calculated in the stability axis system. The angle of sideslip, β, is also measured in the stability axis system, and is in the X_s, Y_s plane while α is measured in the X_s, Z_s plane (or x-z plane, since both are the same) (see Figures 4, 5, and 6).

By rotating the stability axes about Z_s through the angle of sideslip, β, the x axis becomes oriented in the direction of the total Shuttle vehicle velocity, $\bar{V}_p$, relative to air space. If no winds are present, $\bar{V}_p$ will also represent the total Shuttle velocity relative to the non-rotating earth surface.

These forces and moments which are calculated in the stability axis system must be resolved into the body axis system for calculation of the total body axis forces and moments. Also it is assumed that the sideslip angle, β, is small so that $\sin \beta \simeq \beta$ and $\cos \beta \simeq 1$, but the angle of attack, α, cannot be assumed small since the Shuttle assumes fairly high angles of attack.

The equations of motion which were derived according to the above definitions and assumptions are presented here.

Translational Equations in Body-Fixed Coordinates

$$m\dot{U} = -m(WQ - VR) + P_x + X - mg \sin \Theta$$

$$m\dot{V} = -m(UR - WP) + P_y + Y + mg \cos \Theta \sin \Phi$$

$$m\dot{W} = -m(VP - UQ) + P_z + Z + mg \cos \Theta \cos \Phi$$

where

$$V_p = \frac{VRX}{\cos \alpha \cos \beta}$$

$\beta = \sin^{-1} \frac{VRY}{V_p}$ = sideslip angle where $VRY = V - V_{WYB}$

$\alpha = \tan^{-1} \frac{VRZ}{VRX}$ = pitch angle of attack where $VRX = U - V_{WXB}$

$VRZ = W - V_{WZB}$.

Assuming that U is much larger than the components of the wind, $\dot{\alpha}$ may be approximated as:

$$\dot{\alpha} = \frac{\dot{W} - \dot{V}_{WZB}}{U}.$$

Relative Velocities in Earth-Fixed Coordinates

$$\dot{S}_x = U(\cos \Theta \cos \psi) + V(-\cos \Phi \sin \psi + \sin \Phi \sin \Theta \cos \psi) + W(\sin \Phi \sin \psi + \cos \Phi \sin \Theta \cos \psi) + V_{WX}$$

$$\dot{S}_y = U(\cos \Theta \sin \psi) + V(\cos \Phi \cos \psi + \sin \Phi \sin \Theta \sin \psi) + W(-\sin \Phi \cos \psi + \cos \Phi \sin \Theta \sin \psi) + V_{WY}$$

$$\dot{S}_z = U(-\sin \Theta) + V(\sin \Phi \cos \Theta) + W(\cos \Theta \cos \Phi) + V_{WZ}.$$

Dimensionless Angular Rates for Aerodynamic Calculation

$$\bar{Q} = (Q_s c)/(2V_p)$$

$$\bar{R} = (R_s b)/(2V_p).$$

Simplified Rotational Equations with Y Plane Symmetry

$$I_{xx}\dot{P} = +I_{xz}\dot{R} + M_x$$

$$I_{yy}\dot{Q} = M_y$$

$$I_{zz}\dot{R} = +I_{xz}\dot{P} + M_z.$$

Rotational Equations with Y Plane Symmetry

$$I_{xx}\dot{P} = (I_{yy} - I_{zz})QR + I_{xz}(\dot{R} + PQ) + T_x + L$$

$$I_{yy}\dot{Q} = (I_{zz} - I_{xx})RP + I_{xz}(R^2 - P^2) + T_y + M$$

$$I_{zz}\dot{R} = (I_{xx} - I_{yy})\,PQ + I_{yz}(\dot{P} - QR) + T_z + N.$$

Stability Axis Rates

$$P_s = P \cos \alpha + R \sin \alpha$$

$$Q_s = Q$$

$$R_s = -P \sin \alpha + R \cos \alpha.$$

Euler Angle Rates Derived from Body Rates

$$\dot{\psi} = (R \cos \Phi + Q \sin \Phi)/\cos \Theta$$

$$\dot{\Theta} = Q \cos \Theta - R \sin \Phi$$

$$\dot{\Phi} = P + \dot{\psi} \sin \Theta.$$

Dimensionless Angular Rates for Aerodynamic Calculations

$$\bar{P} = (P_s b)/(2V_p)$$

$$\dot{\bar{\alpha}} = (\dot{\alpha} c)/(2\dot{V}_p).$$

Aerodynamic Force Coefficients in Stability Axes

$$C = C_o + C_\alpha \alpha + C_q Q + C_{\delta_e} \delta_e + C_{\delta_r} \delta_r + C_{\delta_a} \delta_a$$

$$C_Y = C_{Y\beta}\beta + C_{Y_r}\bar{R} + C_{Y_p}\bar{P} + C_{Y_{\delta_r}}\delta_r + C_{Y\dot{\beta}}\dot{\beta} + C_{Y_o}$$

$$C = C_\alpha \alpha + C_{\delta_e} \delta_e + C_q \bar{Q} + C_o.$$

Force Equations in Stability Axes

$$X_s = -(\frac{\rho}{2} V_p^2 S) C$$

$$Y_s = (\frac{\rho}{2} V_p^2 S) C_Y$$

$$Z_s = -(\frac{\rho}{2} V_p^2 S) C.$$

Force Equations in Body Axes

$$X = X_s \cos \alpha - Z_s \sin \alpha + \sum_{i=1}^{n} F_{irx}$$

$$Y = Y_s + \sum_{i=1}^{n} F_{iry}$$

$$Z = X_s \sin \alpha + Z_s \cos \alpha + \sum_{i=1}^{n} F_{irz}.$$

Engine Forces

$$P_{xxj} = (P_j \sqrt{1 + \beta_{pj}^2 + \beta_{yj}^2})$$

$$P_y = \sum_{j} (P_{xxj} \beta_{yj})$$

$$P_z = \sum_{j} (-P_{xxj} \beta_{pj})$$

$$P_x = \sum_{j} P_{xxj} \qquad j = 1 \ldots n \quad \text{number of engines.}$$

Aerodynamic Torque Coefficients in Stability Axes

$$C_L = C_{L\beta}\beta + C_{Lp}P + C_{Lr}\bar{R} + C_{L\delta_a}\delta_a + C_{Lo} + C_{L\delta_r}\delta_r$$

$$C_M = C_{M\alpha}\alpha + C_{Mq}\bar{Q} + C_{M\dot{\alpha}}\dot{\bar{\alpha}} + C_{M\delta_e}(\delta_e) + C_{Mo}(\delta_e)$$

$$C_N = C_{N\beta}\beta + C_{Nr}\bar{R} + C_{N\delta_r}\delta_r + C_{No} + C_{N\delta_a}\delta_a.$$

Aerodynamic Torque Equations in Stability Axes

$$L_s = \left(\frac{\rho}{2} V_p^2 \, Sb\right) C_L$$

$$M_s = \left(\frac{\rho}{2} V_p^2 \, Sc\right) C_M$$

$$N_s = \left(\frac{\rho}{2} V_p^2 \, Sb\right) C_N.$$

Aerodynamic Torque Equations in Body Axes

$$L = L_s \cos\alpha - N_s \sin\alpha$$

$$M = M_s$$

$$N = L_s \sin\alpha + N_s \cos\alpha.$$

Total Torques from Engine and Aerodynamics in Body Axes

$$M_x = T_x + L + \sum_{i=1}^{n} L_{R_i}$$

$$M_y = T_y + M + \sum_{i=1}^{n} M_{R_i}$$

$$M_z = T_z + N + \sum_{i=1}^{n} N_{R_i}.$$

Engine Torques in Body Axes

$$T_x = \sum_j [-P_{xxj}\beta_{pj}(Y_{Ej} - Y_{cg})] - P_{xxj}\beta_{yj}(Z_{Ej} - Z_{cg})]$$

$$T_y = \sum_j [P_{xxj}\ (Z_{Ej} - Z_{cg}) - P_{xxj}\beta_{Pj}(X_{Ej} - X_{cg})]$$

$$T_z = \sum_j [P_{xxj}\beta_{yj}(X_{Ej} - X_{cg}) - P_{xxj}(Y_{Ej} - Y_{cg})]$$

$$j = 1, \ldots, n.$$

Flight and Control (Preliminary)

Aileron Control

$$\tau_a\dot{\delta}_a + \delta_a = a_{a_o}\Phi + a_{a_1}P + g_o(S_{y_c} - S_y) + g_1(\dot{S}_{y_c} - \dot{S}_y) + a_{a_2}(\psi_c - \psi) + \delta_{sa}.$$

Elevator Control

$$\tau_e\dot{\delta}_e + \delta_e = a_{e_o}(\Theta_c - \Theta) + a_{e_1}Q + h_o(S_c - S_z) + h_1(\dot{S}_c - \dot{S}_z) + \text{flare} + \delta_{sc}$$

Rudder Control

$$\tau_r\dot{\delta}_r + \delta_r = -a_{r_o}\Phi - a_{r_1}P + a_{r_2}R + a_{r_3}(\psi_c - \psi) + \delta_{sc}$$

$$\gamma = (\dot{S}_z/\dot{S}_x)$$

when $S_z > H_1$, flare = 0 where H_1 = initial flare height

h_2 = final flare height

when $S_z < H_1$, and $\gamma > K_\gamma$, flare = $K_F(\eta_z - \eta_{zc})$

when $\gamma < K_\gamma$, flare = 0.

Reference Position Coordinates

$$S_c = S_x \tan \gamma_z$$

$$S_y = S_x \tan \gamma_y.$$

Throttle Control

$$\delta_T = \delta_{trim} + k_1(S_c - S_z) + k_2(\dot{S}_c - \dot{S}_z)$$

$$k = -.01 \qquad 0 \leq \delta_T \leq 1.$$

Time Lag on Thrust Change

$$\tau_D \dot{P}_J + P_J = \delta_T P_{J_{max}}.$$

Cant Angle Engine Equations

$$\beta_{Pj} = C_{Pj} \text{ (fixed engines)}$$

$$\beta_{Yj} = C_{Yj} \quad (C_{Pj} \text{ and } C_{Yj} \text{ are constant deflections}).$$

These control equations are preliminary and ideal and serve only as a typical type. The program is flexible and can quickly be changed to any guidance and control logic needed. Additional discussions and types of control systems follow later.

Reaction Jet Control Forces

$$\sum F_{irx} = R_{iT} \cos \lambda_x$$

$$\sum F_{iry} = R_{iT} \cos \lambda_y$$

$$\sum F_{irz} = R_{iT} \cos \lambda_z .$$

Reaction Jet Control Moment

$$\sum L_{R_i} = R_{iT}[(Z_{ir}R - Z_{cg}) \cos \lambda_x - (X_{iR} - X_{cg}) \cos \lambda_z]$$

$$\sum M_{R_i} = R_{iT}[(Z_{iR} - Z_{cg}) \cos \lambda_x - (X_{iR} - X_{cg}) \cos \lambda_z]$$

$$\sum N_{R_i} = R_{iT}[(X_{iR} - X_{cg}) \cos \lambda_y - Y_{iR} \cos \lambda_x]$$

$i = 1, \ldots, n$ is the number of engines.

The analog flow diagram of this set of describing equations is shown on charts 1 through 11 in appendix I.

A block diagram of the equations in modular form is presented in figure 7. The format is simple. For example, aerodynamic forces and moments could be used in terms of body axes instead of stability axes, if they were available in that form, by passing or modifying certain steps. The guidance and control equations as presented are very simple, and only indicate where and how they would be incorporated in the loop. This particular module will be subject to more change than any other.

1. Control Systems

One concept for the control system consists of signals to the elevator, ailerons, and rudder. The aileron deflection is determined by a position gain on the bank angle plus a rate gain on the vehicle angular velocity along the x axis, with some error signals for path control. The elevator deflection is determined by a position gain on the attitude angle error plus a rate gain on the vehicle angular velocity along the y axis along with altitude and altitude rate error gains. The elevator also plays an important part in the flare. The rudder position is due to bank angle, vehicle angular position along the X and Z axes and heading error. A first order time delay is included on each of the control surfaces.

The total system may be automatic or may be entirely controlled by the pilot. The throttle input may also be varied manually or may be completely changed automatically to help stay on the glide slope and reach the proper touchdown point. Figures 8 and 9 are typical block diagrams of the system.

During reentry, provision must be made for using a reaction jet control system in this module. Figure 10 is a typical block diagram of a reaction jet system. The system is designed to trade off attitude hold accuracy with reaction jet propellant consumption by inclusion of a "pseudo-rate-modulator" in each channel. The pseudo-rate-modulator implements bang-bang control with deadbands as illustrated by the phase plane plot of the pitch rate versus position error in figure 11. The block diagram illustrates the mixing of signals for six engines mounted on the geometric pitch and yaw axes. Implementation would require a different mixing depending on number of engines and various locations. This was illustrated in the equations for one individual engine where λ_x, λ_y, and λ_z are the angles between the thrust vector and the respective body axes.

2. Overall Simulation Concept

The portion of the simulation discussed so far is general and is needed for both manual and automatic control studies. Its implementation for initial studies was made on an analog computer. A hybrid implementation is in process which will allow the incorporation of altitude, Mach number effect, nonlinear aerodynamics, winds, etc. The winds can be used as detailed measured winds, discrete winds, or statistical winds. Logic for collating and interpreting output data can be built into the digital portion of the hybrid. Strip charts can be used as output.

Figure 12 is a schematic diagram illustrating the flexibility of the studies. The left-hand series of blocks is the analog or hybrid simulation of the vehicle dynamics, control, and disturbances. Through proper interface (shown as a switch), the vehicle simulation can be used with the cockpit and visual simulation or run by itself for special studies. Since only one dynamic simulation has to be developed for both manned and unmanned studies, this approach is very practical. The cockpit and visual displays are discussed in the following sections.

III. SIMULATOR COCKPIT AND DISPLAYS

The previous sections have discussed the basic philosophy and the dynamics and control portion of the simulation implemented on the analog or hybrid computer. This section deals with the man-machine interface.

Man's ability to act intelligently to the unexpected has made him a very important element in space vehicles; therefore, it has become necessary to include him in the vehicle development studies--to design the system so that man becomes an integral part. This is best accomplished using the man-machine type of simulators.

The Simulation Branch, MSFC, first became involved in man-machine simulators in 1962 and since that time has grown quite rapidly in its capabilities (Figure 13). All computers and simulation equipment terminate at central trunking stations to provide maximum adaptability and flexibility for engineering studies (Figures 14 and 15). The Space Shuttle Simulator, which is presently operational, represents several years of development in the simulation field. Figure 16 is a block diagram of this system.

Out-of-the-window views are provided by the Link SMK-23 visual unit. The SMK-23, built by Link Division of General Precision, Inc. for use by the Air Force in pilot training and keeping the pilots proficient in landing on airport runways, consists of a camera and model unit, and a projector and screen which provides the crew station simulator operator a view of the terrain he is flying over. The SMK-23 includes a 3000-1 scale model (in three dimensions) of Castle Air Force Base, California. This terrain model is installed on a large roller belt, 3.66 m wide and 8.23 m long. Table 1 gives the characteristics of the SMK-23.

Table 1. SMK-23 Terrain and Landing Visual Simulator

Model Scale	Translation				Rotation			
		Range	Velocity	Accel.		Angle	Rate	Accel.
3000:1	X	20921 m	125 m/s	274 m/s^2	Pitch	±.436 rad	±1.12 rad/sec	±1.745 rad/sec^2
	Y	9656 m	131 m/s	265 m/s^2				
	Z	7.5... 600 m	14.6 m/s	152 m/s^2	Roll	1.047 rad	± 3 rad/sec	±8.73 rad/sec^2
					Yaw	±15.7 rad (±2 1/2 turns)	± 2 rad/sec	±8.73 rad/sec^2

The television camera scans this three-dimensional model with an optical probe that provides pitch, roll and yaw. Altitude is simulated by moving the camera and pickup lens above the terrain model to represent a maximum visual altitude capability of 610 meters. The minimum altitude capability is approximately 6.7 meters which represents the eye level of a pilot in a large aircraft with its wheels touched down on the runway. To provide for such a condition the entrance pupil of the optical probe is less than .0025 m from the model. To allow for this close approach of the optical probe, the initial element in the optical chain is only about two millimeters in diameter. The camera used provides field sequential color.

The picture obtained from the camera and model is provided by means of a video link to an Eidophor Projector located at the crew station simulator. Figure 17 is a projection of this picture on the screen out the pilot's and copilot's windows. Specifications for the SMK-23 are given in Table 1.

The crew station simulator used for the present Shuttle studies consists of a two-man general purpose device. It was designed under MSFC contract by the Boeing Aerospace Division in Seattle. The crew station, which evolved from prior experience at MSFC, features a modular concept. Prior work with simulators showed the difficulty in rearranging cockpit instrument panels, seating, and controls. The General-Purpose Two-Man Crew Station was therefore designed for maximum flexibility. The major items of the cockpit can be incorporated in building-block fashion to represent a variety of vehicle concepts. The enclosure is not rigidly attached to the cockpit floor, but can be lifted off and a different enclosure installed to represent a different vehicle. Also, the instrument panel is not attached to the enclosure but rather to the floor; therefore, the instrument panel can be easily removed, and a complete instrument panel arrangement can be installed. Likewise, seating can be changed.

The connections to the computer are via an interface console. The console includes a removable patch board so that once the instrument connections are wired to a program they can be readily changed just by inserting another removable patch board and installing on the cockpit floor the corresponding instrument panels.

Because of these features, the configuration of the vehicle represented in the crew station structure can be changed in a matter of a few hours. At the same time, the computer-program would be changed. Thus, the vehicle simulation can be completely changed in about one day.

At present the instrumentation consists of standard aircraft instruments such as the Lear-Seigler Model 4060P Attitude-Director Indicator, Gyro Magnetic Compass, Altimeter, Rate-of-Climb Indicator, Mach Number Indicator and Airspeed (Knots) Indicator, all of which are synchro driven. Other meters of the d'arsonval type are used to read out variables which do not require such an accurate interpretation. A number of indicator switches are available for the operator to use for putting in various operating conditions such as the autopilot.

Figure 18, a picture of the interior of the cockpit, shows the instruments, and Table 2 lists the present cockpit characteristics.

Table 2. Cockpit Characteristics

1. Stick Control of Aileron, Elevators, and Rudder if Desired
2. Rudders
3. Throttle
4. Instrumentation
   - a) Glide Slope
   - b) Air Speed Indicator
   - c) Altimeter
   - d) Rate of Climb
   - e) Three-axis Attitude Indicator
   - f) Directional Gyro
   - g) Roll Angle
   - h) Pitch Angle
   - i) Yaw Angle
   - j) Percent of Thrust
   - k) Mach Number
5. Headphones and Speaker
7. Wind Switch
8. Panel Lights
9. Fixed Base
10. Turn and Slip Indicator
11. Loads Instrument

Although the Shuttle Simulator is quite adequate for the present level of studies, the system must be improved to add more realism as the program becomes more sophisticated. Visual cues must be improved and motion should be added to provide more typical cues for the simulator pilot. Man's reactions must be evaluated in as nearly an actual environment as possible; only then can his full potential be properly incorporated.

Equipment now available which may be added to the simulation as the simulation develops is described in the following paragraphs.

A. Link Six-Degree-of-Freedom Motion System

The 6DOF motion system, developed for simulation of high performance aircraft by Link Division General Precision, is capable of providing independent motion in six degrees of freedom to a motion platform. This is achieved by simultaneous and yet independent operation of six hydraulic actuators, arranged in three bipod pairs, between the platform and floor. For normal motion of the platform, it is necessary for all six actuators to operate simultaneously. Operating specifications for the 6DOF motion system are shown on Table 3. A picture of the unit is shown in Figure 19.

Table 3. Six-Degree-of-Freedom Motion System

Payload: 20,000 pounds

Delivery to MSFC: August 1969

	Position	Rate	Acceleration
Pitch	+.524 rad, -.349 rad	±.262 rad/sec	±.436 rad/sec^2
Roll	±.384 rad	±.262 rad/sec	±.837 rad/sec^2
Yaw	±.558 rad	±.262 rad/sec	±.837 rad/sec^2
Vertical	.991 m up, .762 m down	±.61 m/sec	± 0.8 g
Lateral	±1.219 m	±.61 m/sec	± 0.6 g
Longitudinal	±1.219 m	±.61 m/sec	± 0.6 g

B. Farrand "Pancake" Virtual Image Lens System

The "pancake" lens system is a non-pupil-forming infinity image system that provides a 1.047 meter display. It will not interfere with most cockpit configurations because no obstructions or inclined beam splitters exist forward of the collimating eyepiece mirror. It is termed the "pancake window" because of its minimal depth and, therefore, relatively flat appearance. The eye relief is approximately 160 percent of the focal length and the physical thickness is only about 50 percent of the focal length. An assembly drawing is shown in Figure 20.

C. Dalto DEC M-15 Model Unit

Dalto Electronics Corporation is under contract to deliver to MSFC a DEC M-15 model unit in March 1971. It will consist of a servo-driven gantry for three-degree-of-freedom translational motion of a television camera over a fixed terrain model.

The model will be 4.572 meters by 12.192 meters and will represent the air strip at Cape Kennedy with typical surrounding terrain. The model will also include known landmarks to assist the simulator pilots in navigation. A conceptual drawing of the unit is shown in Figure 21.

The gantry is positioned by D-C servos utilizing zero backlash traction drives which will result in high positional accuracy with excellent repeatability. Performance capabilities are given in Table 4.

Table 4. DEC-M15 (Dalto)

Model 4.57 m x 12.19 m
Model Scale 2500:1

	Position	Velocity	Acceleration
X	30,480 m	518 m/sec	76 g
Y	±4,572 m	61 m/sec	40 g
Z	7.9 m to 1524 m	60.96 m/sec	6 g

D. Adage Graphics Terminal Computer System

The Adage Graphics Terminal Computer System (AGT-30) can display three-dimensional information with rotation and translation in all three axes which could provide flexibility in studying scope-type displays for the Space Shuttle. The digital processor is a general purpose digital computer with extensive transfer logic and addressing capability. It features an SK thirty-bit memory with a two-microsecond memory cycle time and a one-microsecond register to register transfer. Its peripherals include a magnetic tape, a set of discrete function switches, a light pen, and a "joystick" (Figure 22).

The hybrid array solves a transformation matrix of the following form for output to the vector generator:

$$\begin{vmatrix} X \\ Y \\ Z \end{vmatrix} = \begin{vmatrix} X^1 \\ Y^1 \\ Z^1 \end{vmatrix} \begin{vmatrix} A_{11} & A_{12} & A_{13} \\ A_{21} & A_{22} & A_{23} \\ A_{31} & A_{32} & A_{33} \end{vmatrix} + \begin{vmatrix} DX \\ DY \\ DZ \end{vmatrix}$$

(Analog) (Digital)

The vector generator takes the desired end points of vectors and converts them to proper signals for driving the display scope. Some typical measures of performance are as follows:

1) Up to 4500 2D short vectors (1.27 centimeters) at 40 frames/sec.

2) Up to 1660 3D vectors with up to 7.62 centimeter components, 800 with 17.78 centimeter components, or 640 with 25.4 centimeter components at 40 frames/sec.

The character generator allows 64 alphanumeric characters to be drawn rapidly under hardware control.

The AGT-30 is interfaced to an EMR-6050 digital computer. This gives much flexibility and capability because the EMR-6050, in addition to being a general purpose digital computer, is linked as a hybrid system to several analog computers.

There is a full set of software on the AGT-30 including a magnetic tape operating system, assembler, compiler, and display software.

The use of this equipment will allow various displays on a cathode ray tube available to the pilot to aid in his "man-in-the-loop" role or only as a monitor. Figures 23 and 24 are typical examples of some displays that could be portrayed on the cathode ray tube.

IV. DYNAMICS AND CONTROL STUDIES

The present Space Shuttle configuration consists of two reusable stages, each of which must have manned capability. The basic performance requirements are in the Level I and Level II specifications. Level I specifications call for (a) go-around capability for booster and orbiter with air breathing engines (ABES), (b) landing capability with and without ABES, (c) ferrying capability of all vehicle stages between airports, and (d) intact abort after lift-off.

Level II specifications state that trade studies shall be performed to prove or disprove the desirability of (a) pilot control of landing (booster and orbiter) under FAA Category II landing specifications, (b) autopilot and navigation aids similar to systems used in commercial aircraft.

These requirements, along with the various mission phases, fairly well dictate the studies that need to be made. Although the simulation can be used with or without the cockpit, this system will manily be used with the cockpit.

Since the main purpose of this report is to present the characteristics of simulation, detailed dynamics and control studies are not discussed. Some of the dynamics and control studies to be made in the future are listed below.

1. Manual Control Studies

   a. Ascent Abort (Prior to Reentry)

      (1) Determine preliminary control system requirements (feel characteristics, displayed information, engine and surface accelerations, rates and displacements, augmentation requirements, etc.) for manual takeover for abort.

      (2) Verify that handling qualities are acceptable for the situation.

      (3) Verify capability to manually fly through winds, gusts, and transients resulting from malfunction without structural overstress.

(4) Verify guidance, navigation and control compatibility in the presence of a navigation error model such that manual control can be used to return vehicle stages to an acceptable site following abort.

b. Reentry

(1) Determine preliminary control and display system requirements for manual piloting during reentry.

(2) Determine preliminary RCS propellant budget for piloted control of reentry.

(3) Verify piloting path load factor and heating control in conjunction with the guidance and navigation system and its error model.

(4) Determine piloting technique for transition maneuver.

c. Cruise

(1) Determine preliminary control and display requirements.

(2) Verify handling qualities.

(3) Determine gust response.

(4) Verify guidance, navigation and control compatibility, including navigation error model.

d. Landing

(1) Determine preliminary control and display requirements necessary to landing vehicle.

(2) Evaluate landing aids.

(3) Verify handling qualities, control power, and pilots ability to flare and land vehicle.

(4) Determine gust responses and evaluate decrab abilities.

(5) Evaluate landing techniques (i.e., elevon-canard control interaction) including navigation error model.

2. Automatic Control Studies

a. Reentry

(1) Determine optimum system monitoring and display.

(2) Determine ride qualities.

b. Cruise

(1) Determine winds and gust response and verify ride qualities.

(2) Determine optimum system monitoring and display.

c. Landing

(1) Determine ride qualities

(2) Determine optimum system monitoring and display.

3. Manual versus Automatic

a. Ascent Abort and Reentry

Trade-off pilot lag and decreased error resolution versus logic complexity to achieve pilots adaptability.

b. Landing

Trade-off pilot lag and decreased error resolution versus complexity of autopilot to correct navigation and landing aid instrument and system errors.

V. FUTURE PLANS AND CONCLUSIONS

The present simulation model has been shown in detail. It includes:

(1) Cruise and Landing Phases

(2) Linear Aerodynamics

(3) Constant Coefficients

(4) Variable Thrust

(5) Sinusoidal Wind Gust Model

(6) Control through Aerodynamic Surfaces

(7) Simple Malfunction for Manual Takeover

Since this model has some limitations, such as constant coefficients and linear aerodynamics, and since it is also limited to the landing phase of the mission, a hybrid simulation of the vehicle dynamics and control is being developed. The characteristics of this model are as follows:

(1) Reentry, Cruise, and Landing Phases of Flight

(2) Nonlinear Time Varying Coefficients

(3) Control Forces from Aerodynamic Surfaces and RCS

(4) Actual Wind Profiles

(5) Nonideal Control Effects (Lags)

(6) Navigation Error Model

(7) Statistical Evaluation Techniques

- (a) Footprint Density
- (b) Landing Loads Envelope
- (c) Performance Dispersions (Flyback Fuel and Go-Around)

(8) Malfunctions for Manual Takeover

(9) Landing Gear Deployment Model

(10) Automatic Landing Simulated System Including Flare

(11) Moving Base Option

(12) Runway Roughness

(13) Ground Effects

(14) Flaps, Spoilers, etc.

These various subsystems and effects will be programmed in modular form so that the system can be developed in steps and used at any stage of development.

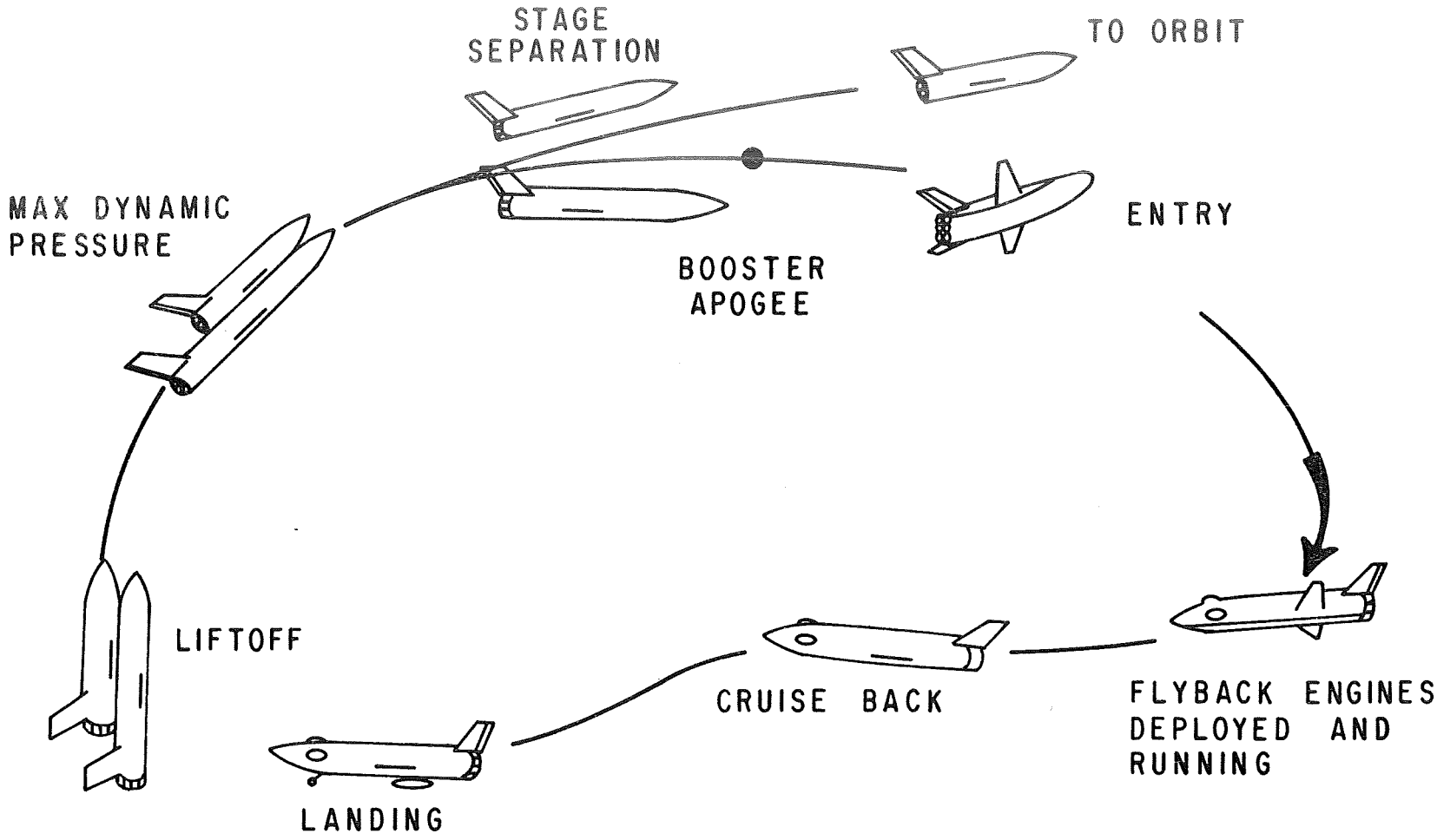

FIGURE 1: FLIGHT PROFILE

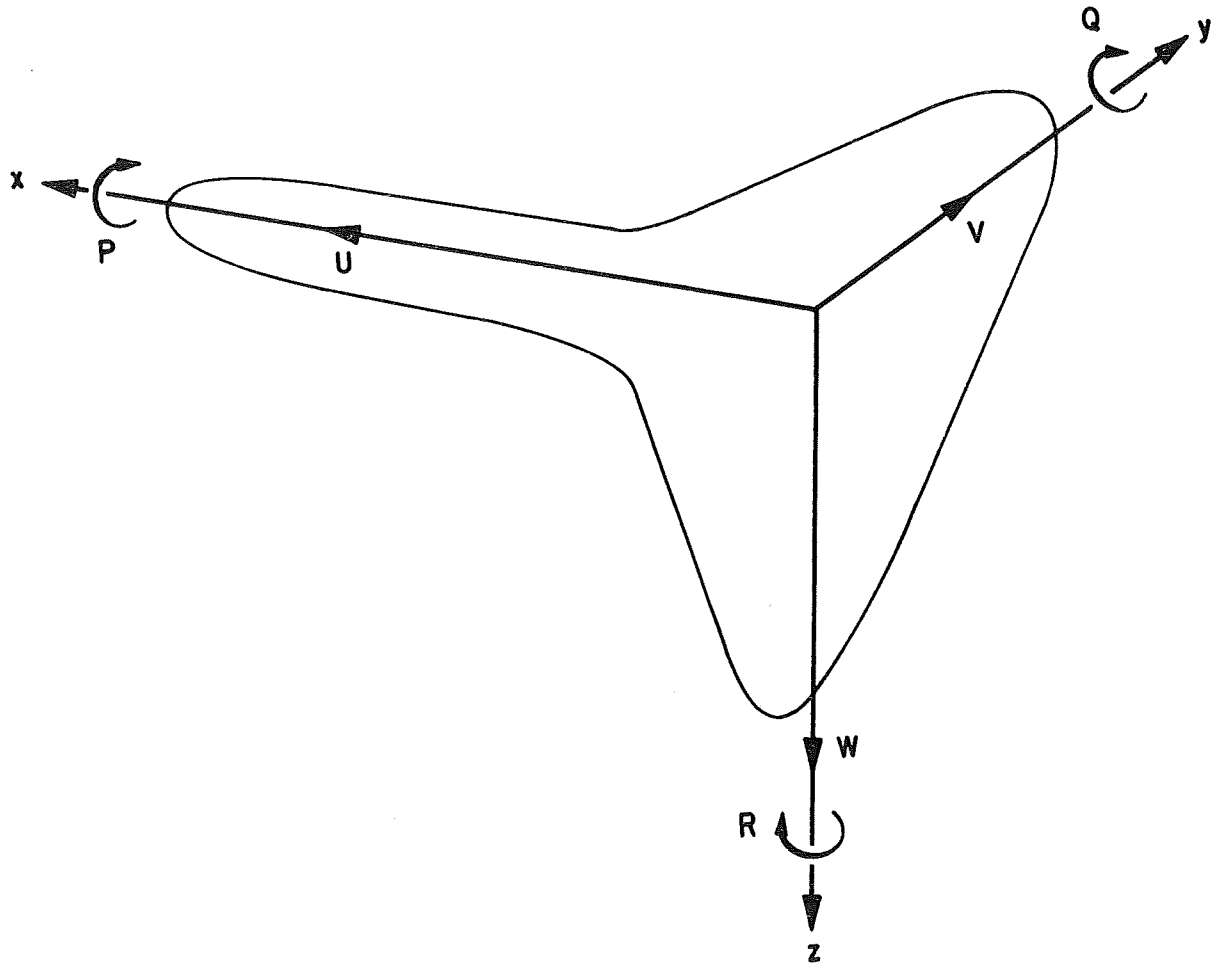

FIGURE 2: COÒRDINATE SYSTEM TRANSLATIONAL AND ROTATIONAL VELOCITY COMPONENTS ALONG THE BODY AXES

EULER ANGLES (YAW, PITCH, ROLL ORDER)

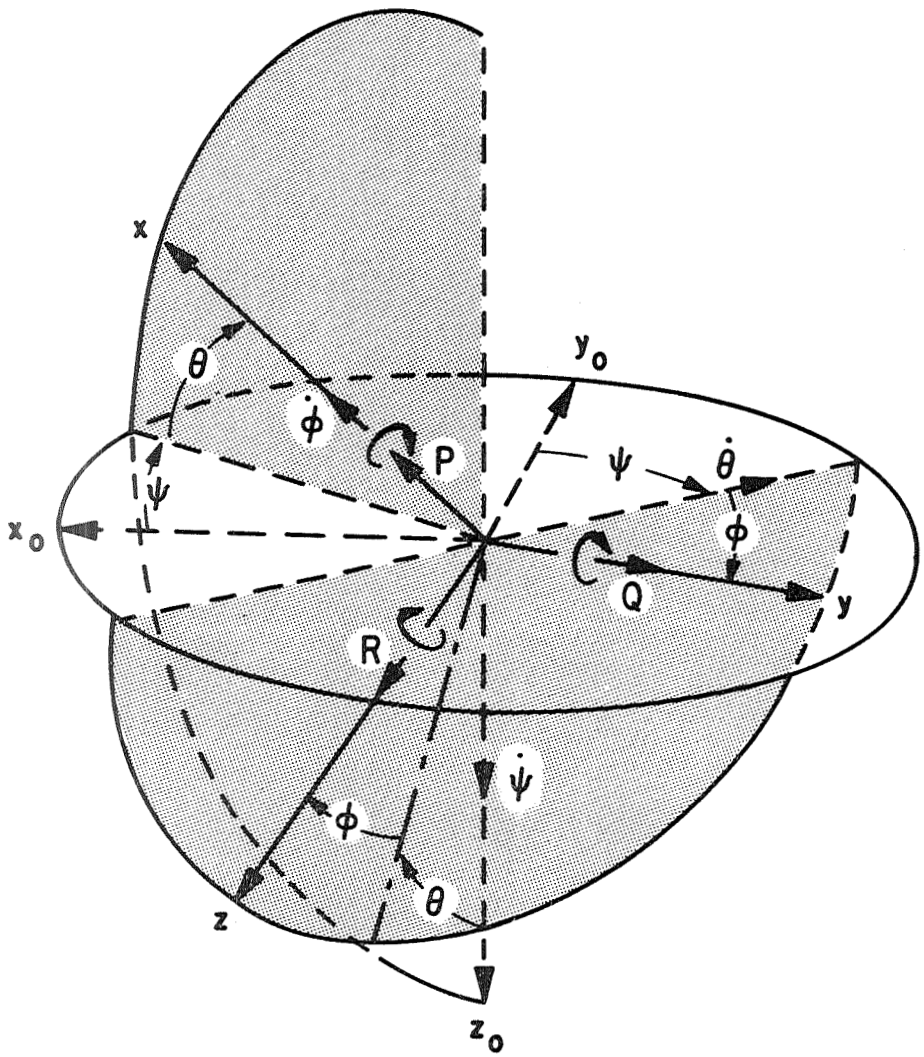

FIGURE 3. COORDINATE SYSTEM

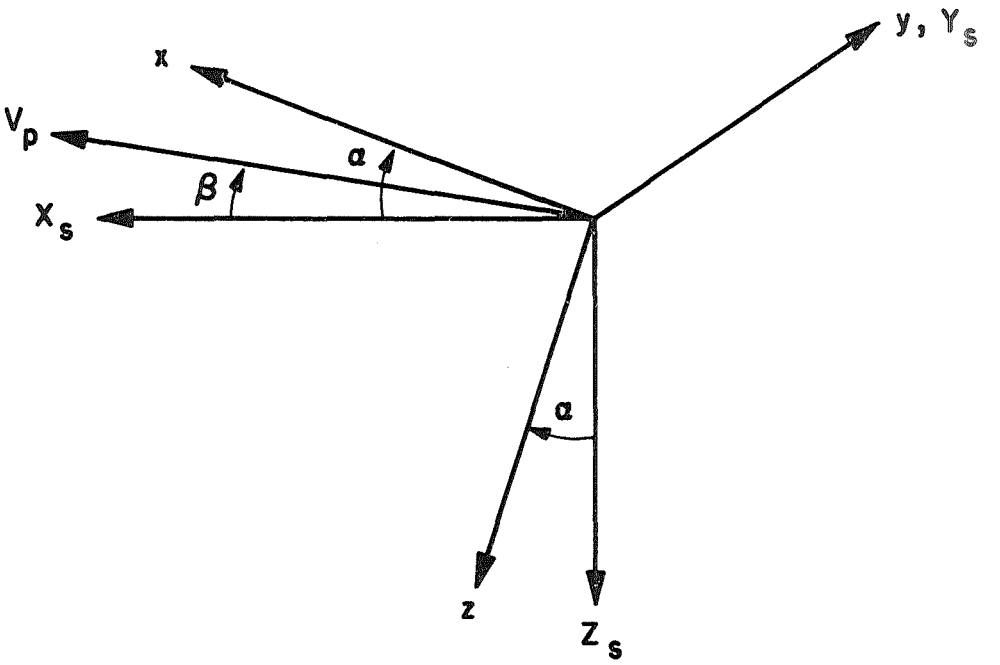

V_p Total Aircraft Velocity

x, y, z Body Axis

X_s, Y_s, Z_s Stability Axis

α Angle of Attack

β Angle of Sideslip

FIGURE 4: STABILITY AXES

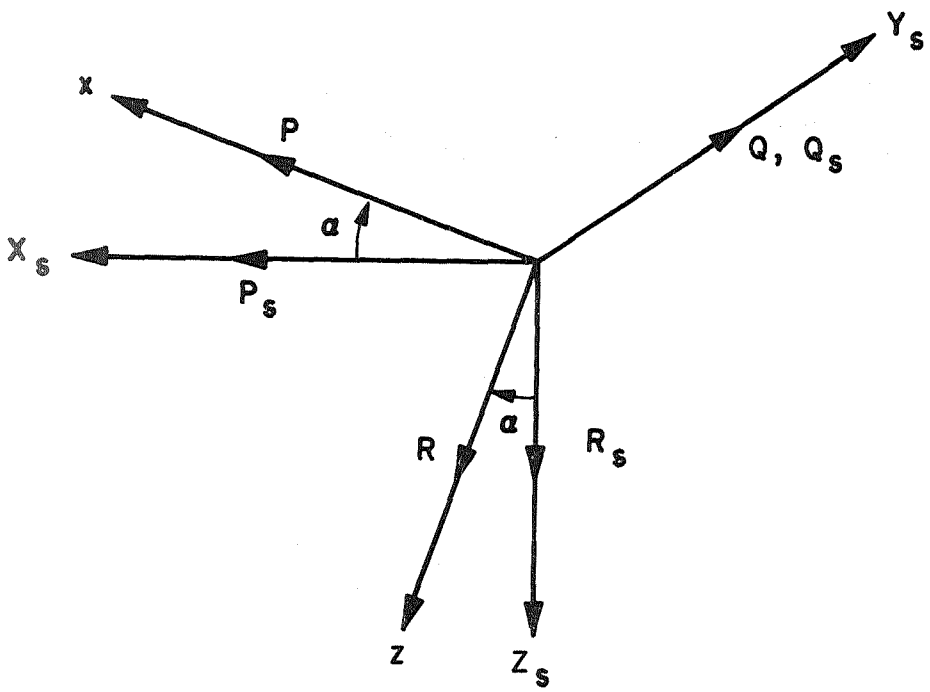

FIGURE 5: BODY-AXIS ANGULAR RATES ALONG STABILITY AND BODY AXES

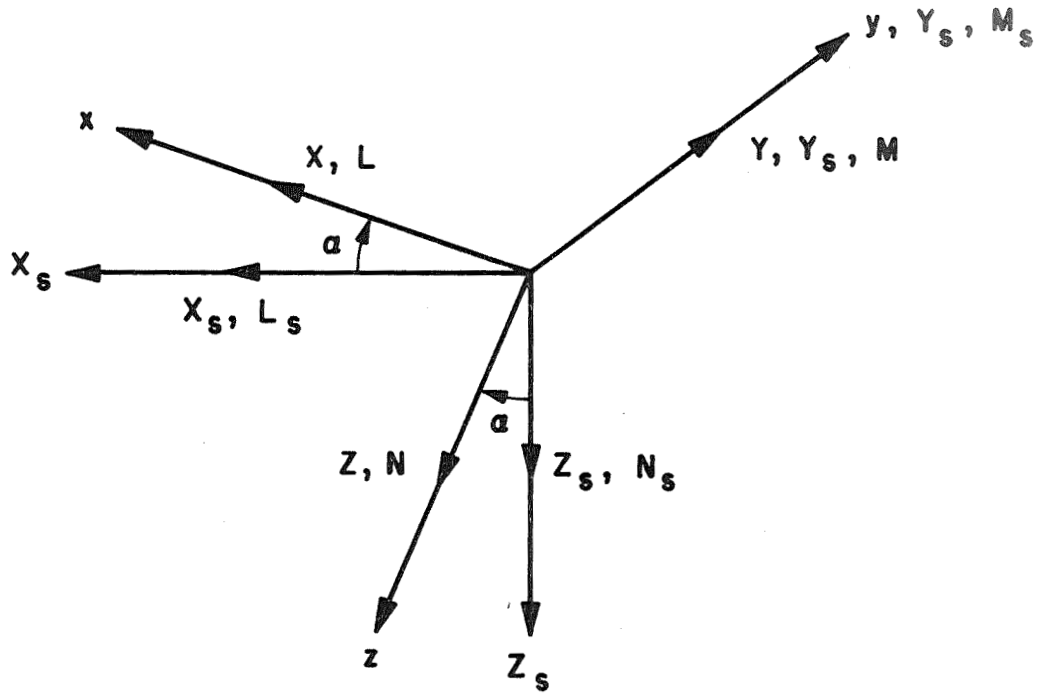

X, Y, Z Forces

L, M, N Moments

FIGURE 6: RESOLUTION OF AERODYNAMIC FORCES AND MOMENTS FROM STABILITY TO BODY AXES

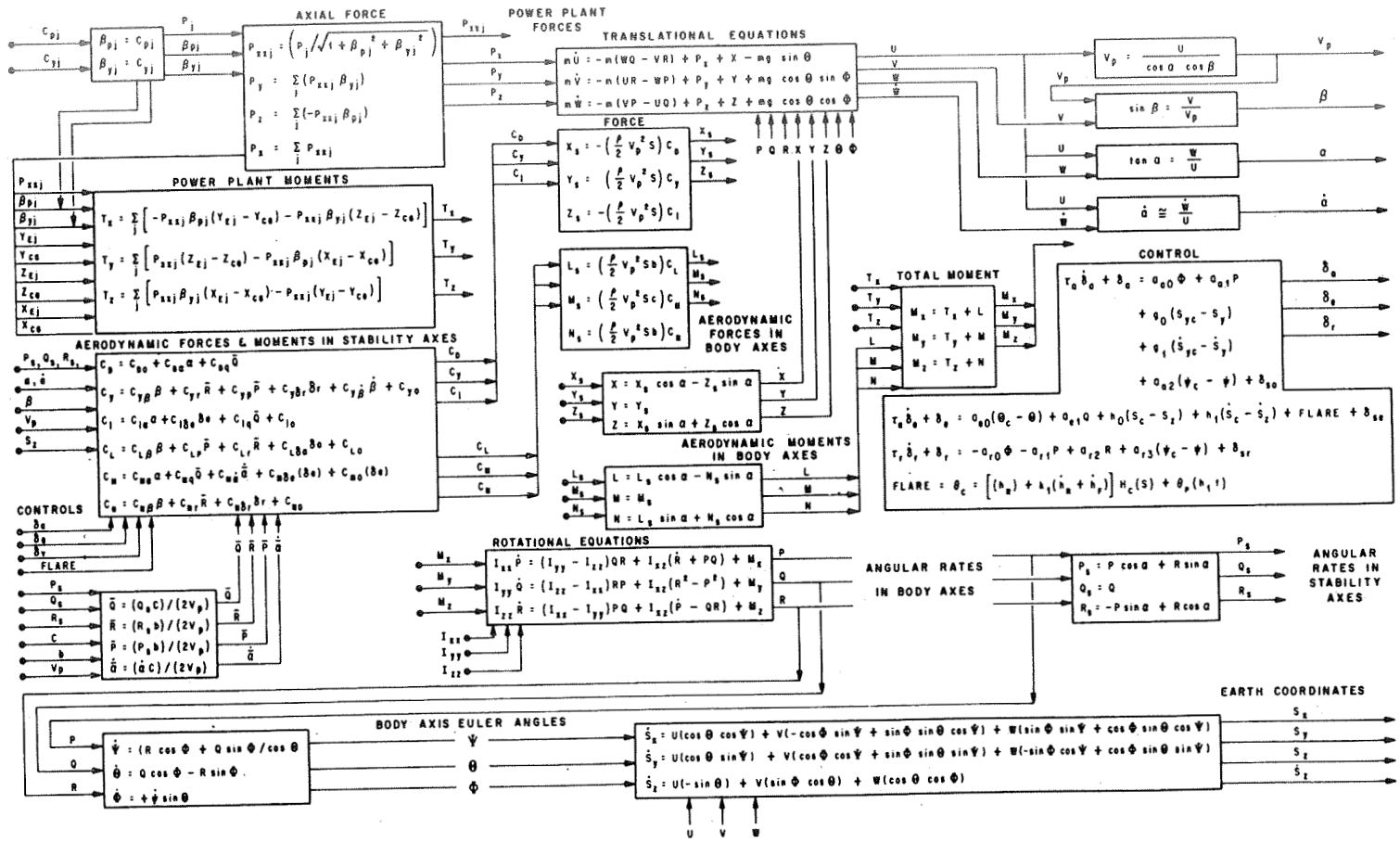

FIGURE 7: BLOCK DIAGRAM OF THE FLIGHT EQUATIONS SOLVED IN BODY AXES

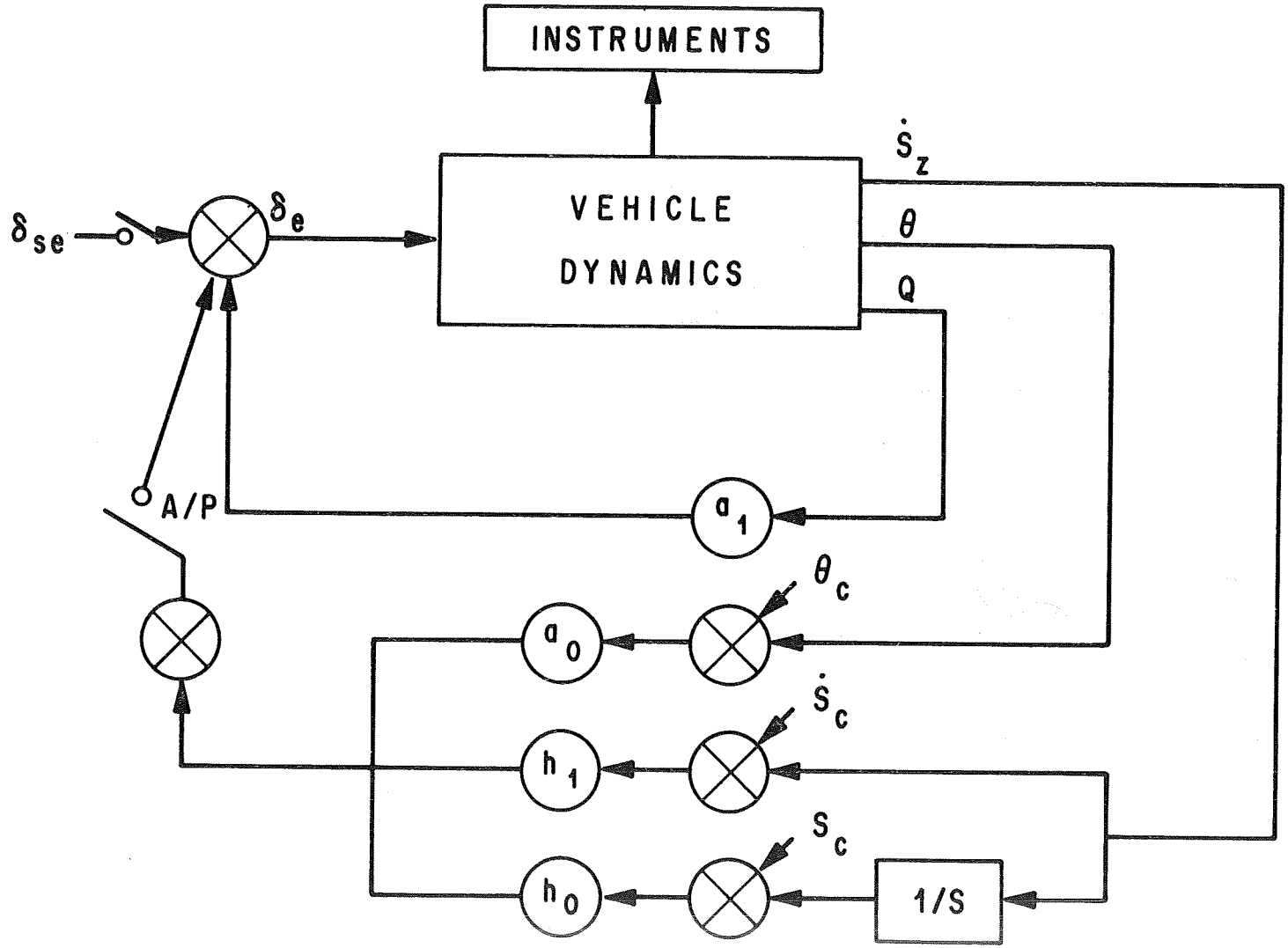

FIGURE 8: LONGITUDINAL CONTROL SYSTEM

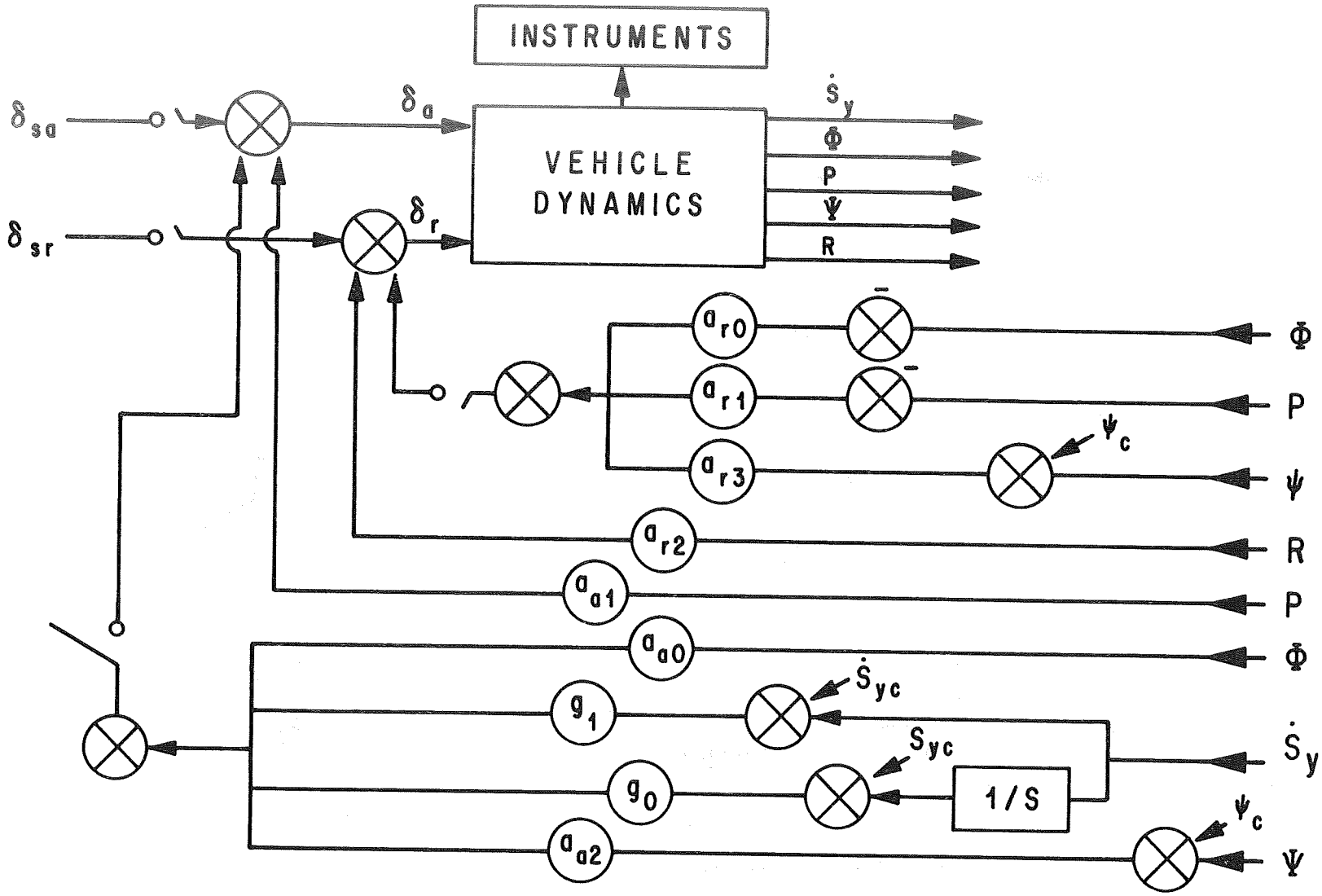

FIGURE 9: LATERAL DIRECTIONAL CONTROL SYSTEM

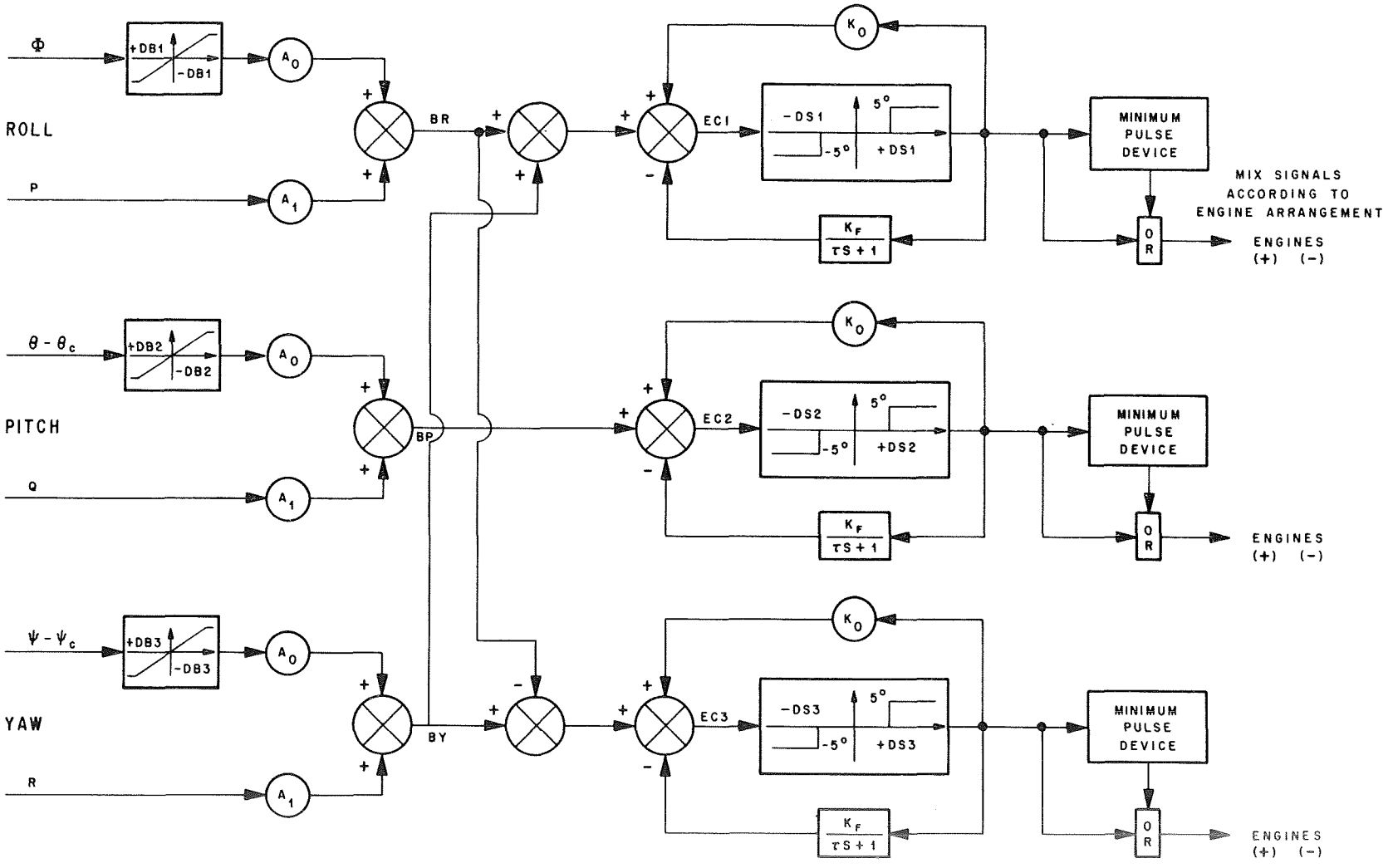

FIGURE 10: CONTROL SYSTEM BLOCK DIAGRAM

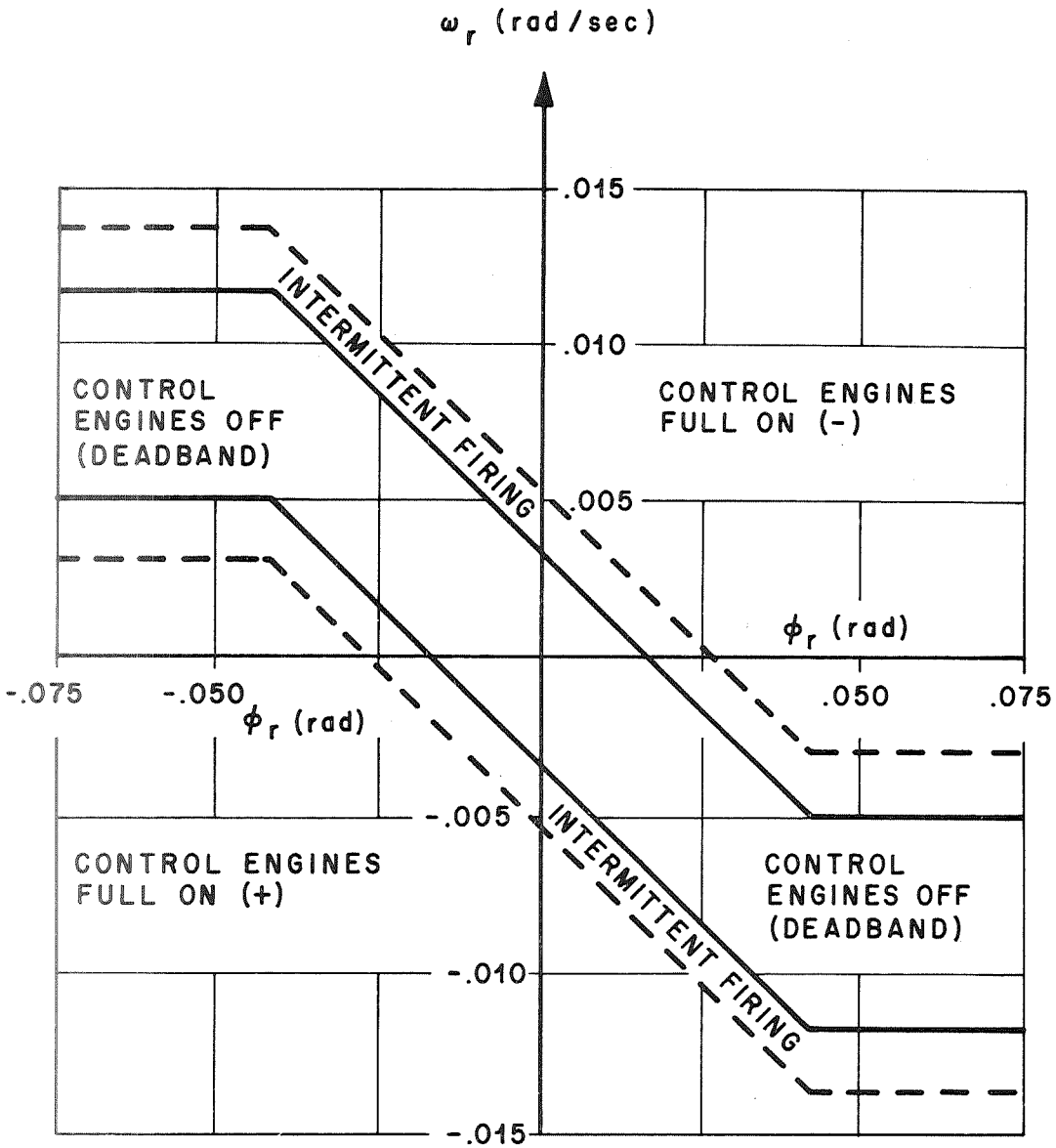

FIGURE 11: PHASE PLANE DIAGRAM FOR THE REACTION JET CONTROL SYSTEM

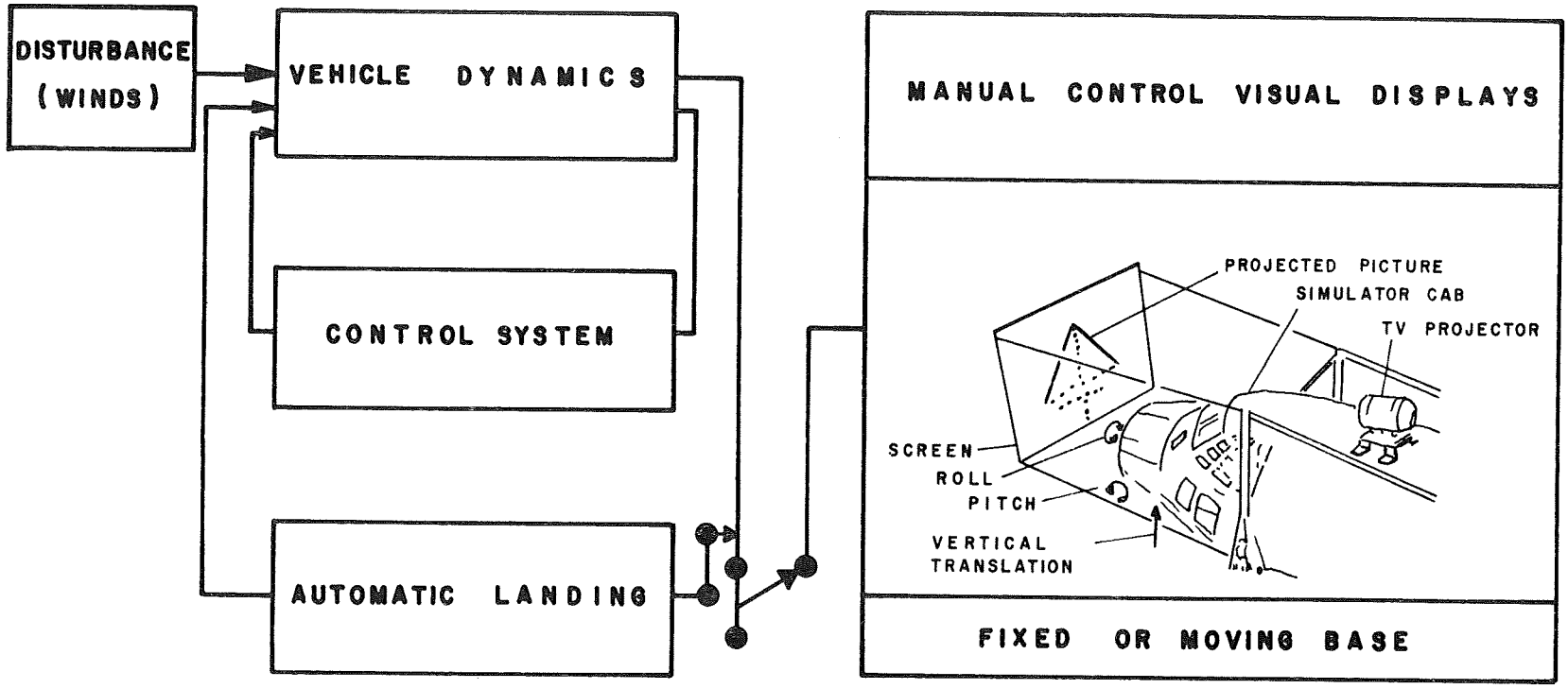

FIGURE 12: CRUISE-REENTRY-LANDING STUDIES

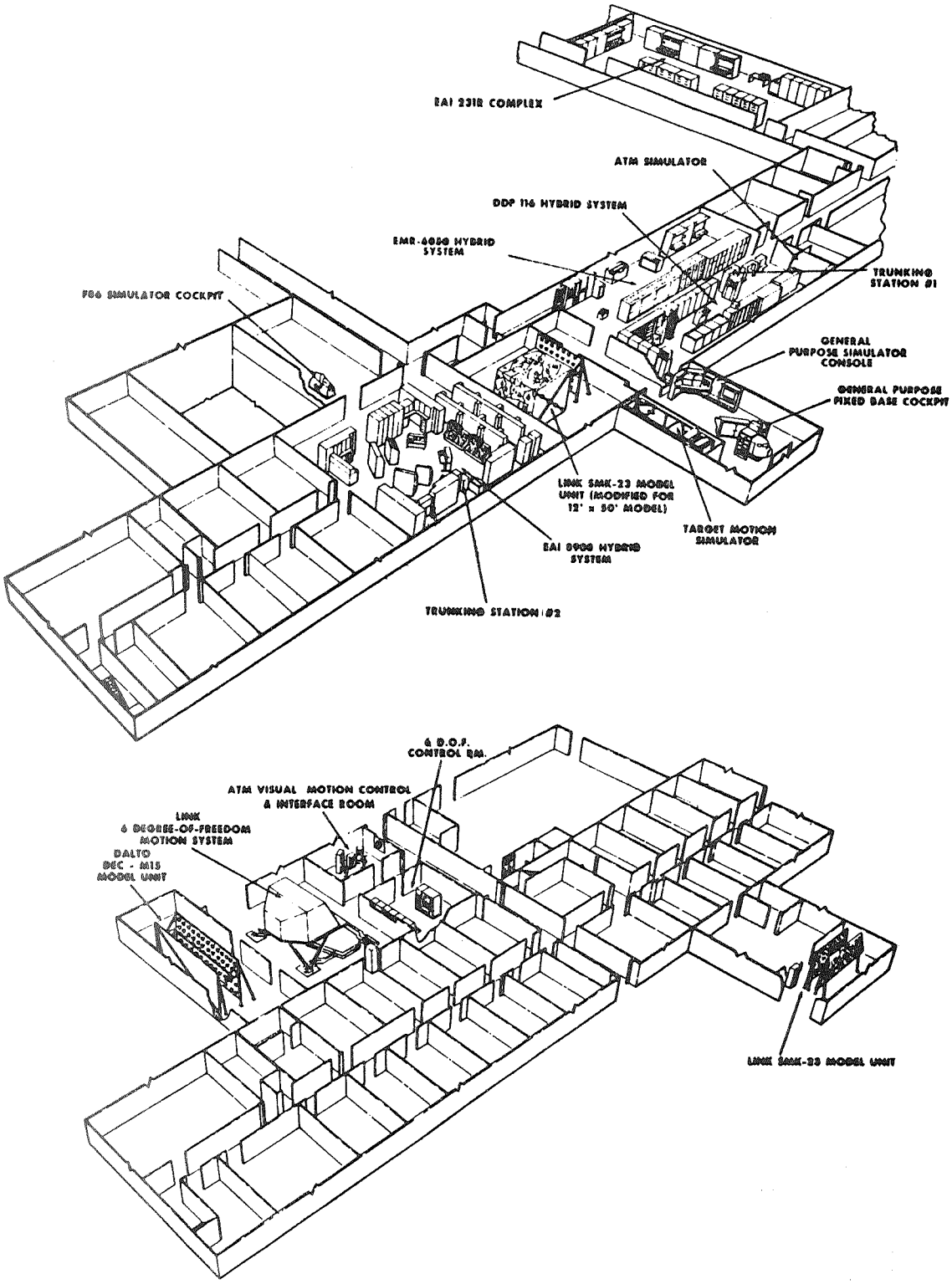

FIGURE 13: MSFC COMPUTATION LABORATORY PHYSICAL SIMULATION FACILITY

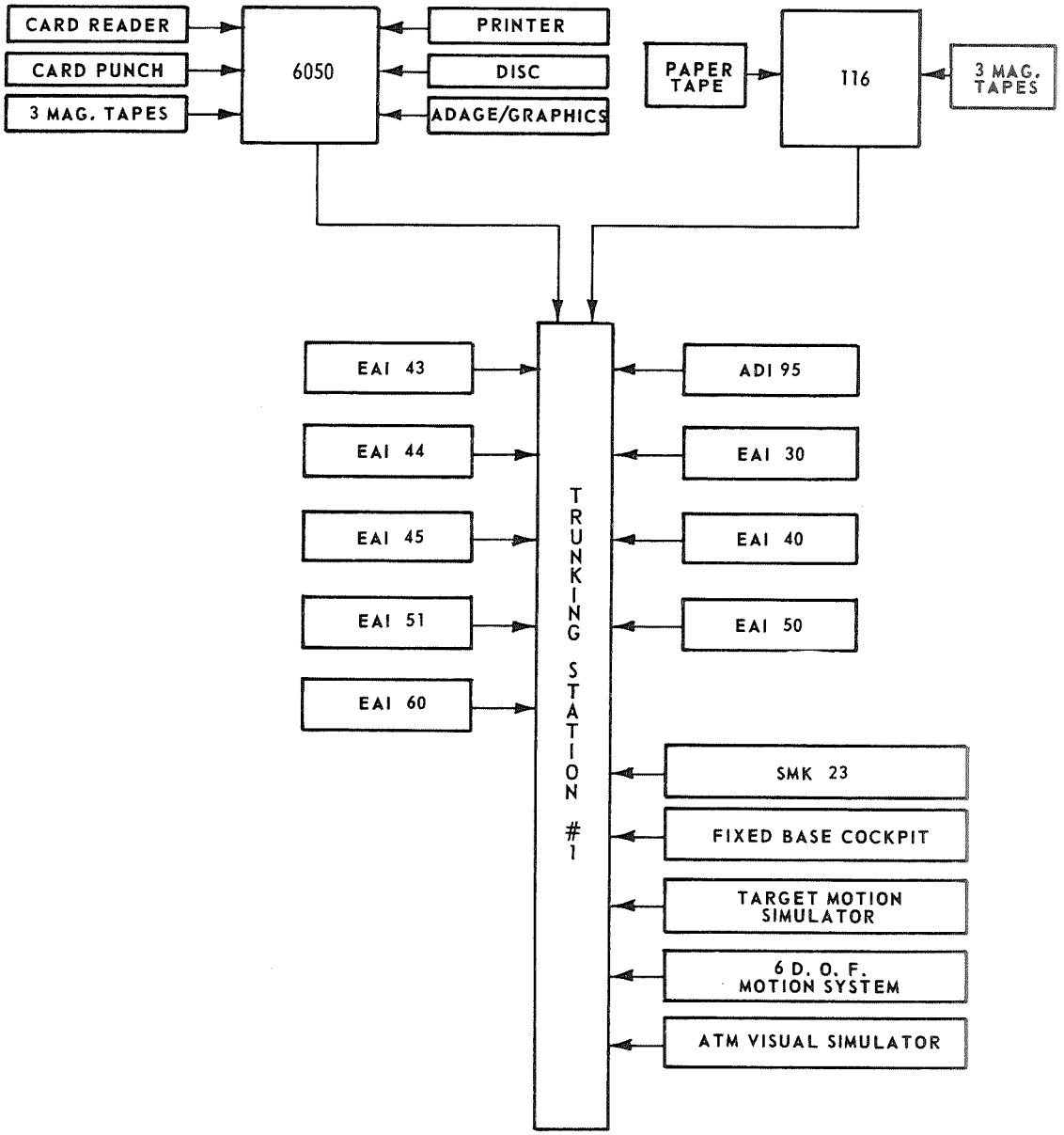

FIGURE 14: CENTRAL TRUNKING STATION GENERAL LAYOUT

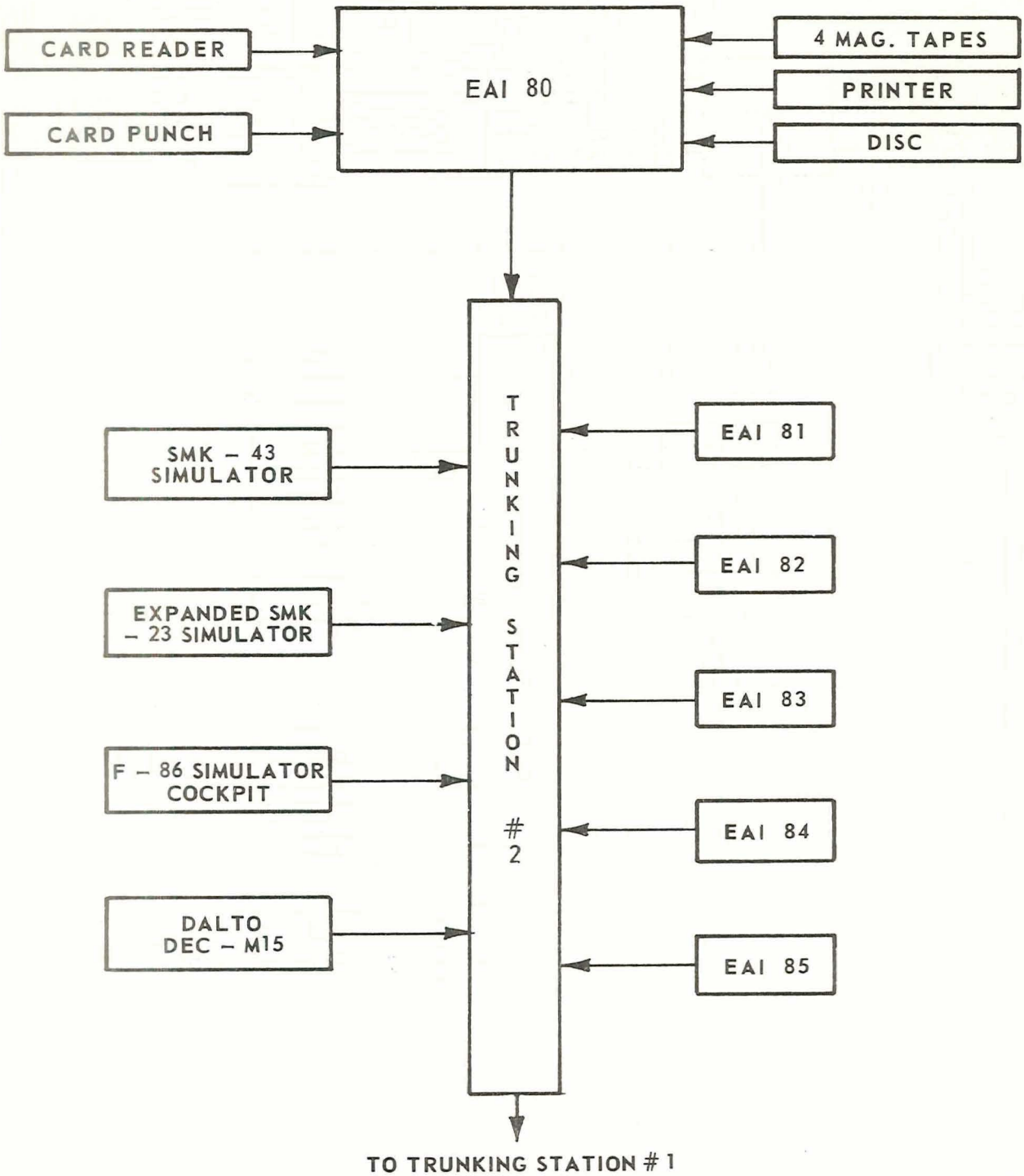

FIGURE 15: CENTRAL TRUNKING STATION SIMULATOR AND COMPUTER LAYOUT

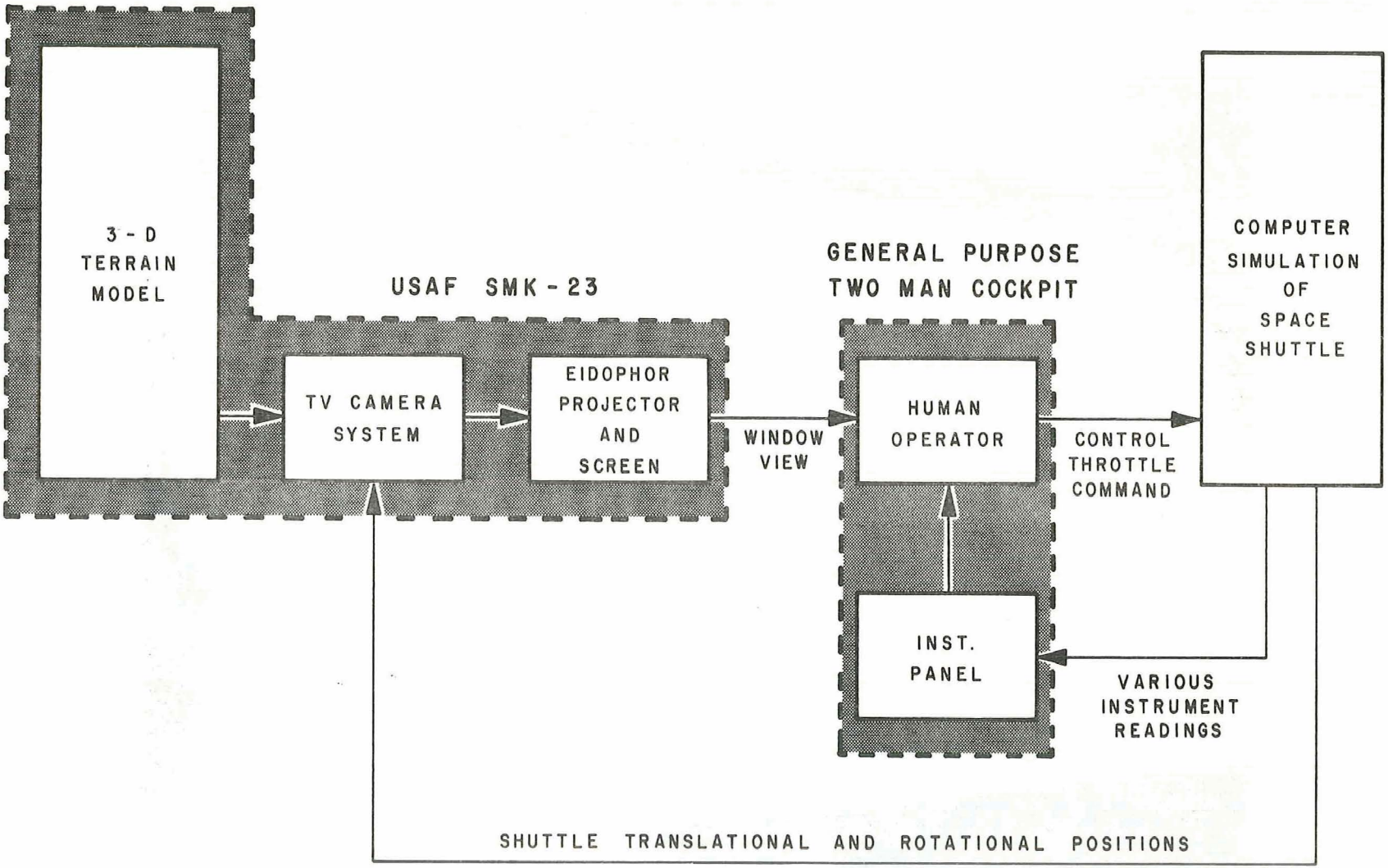

FIGURE 16: SIMULATOR APPLICATION FOR A SPACE SHUTTLE

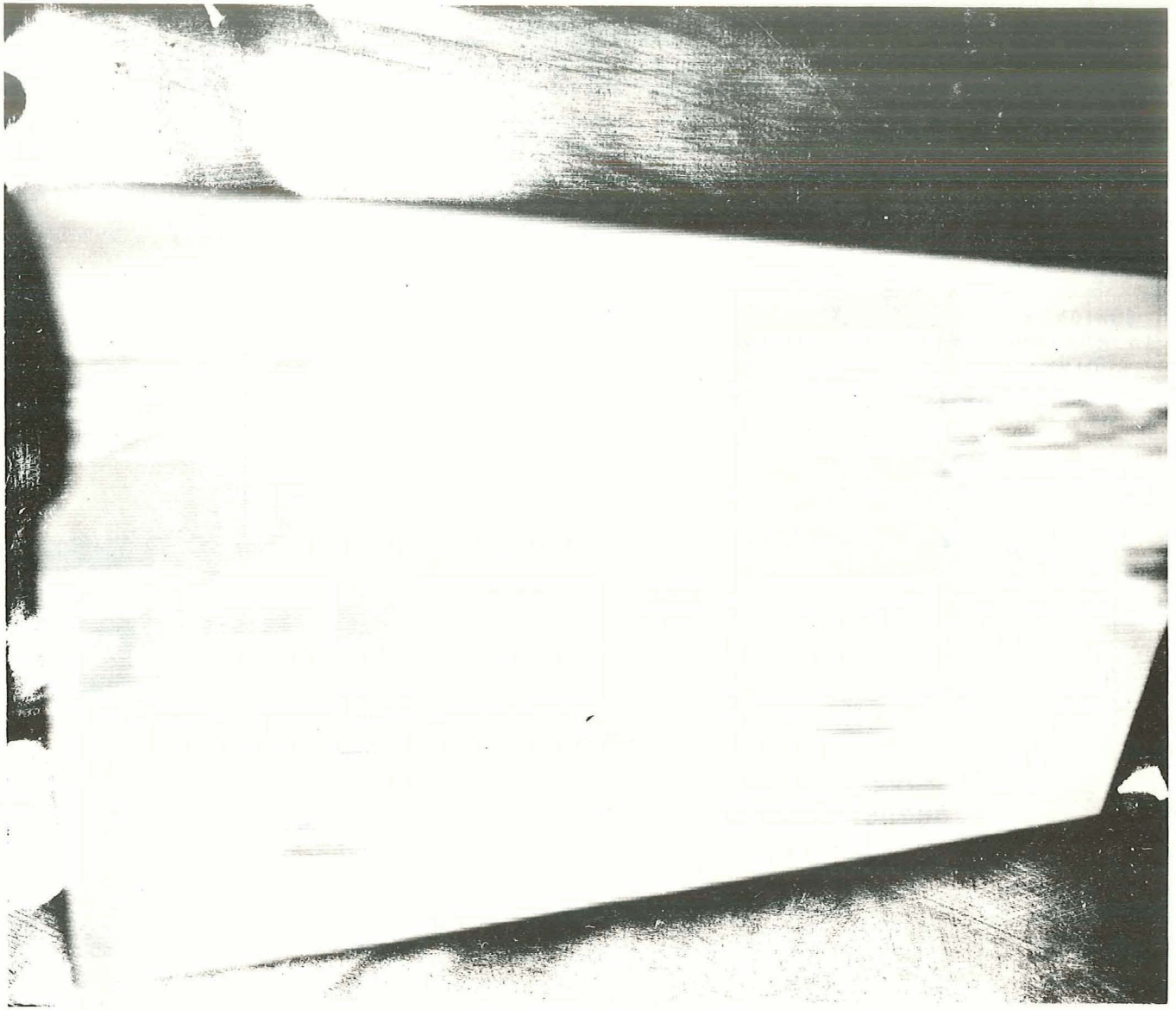

FIGURE 17: OUT-THE-WINDOW RUNWAY DISPLAY

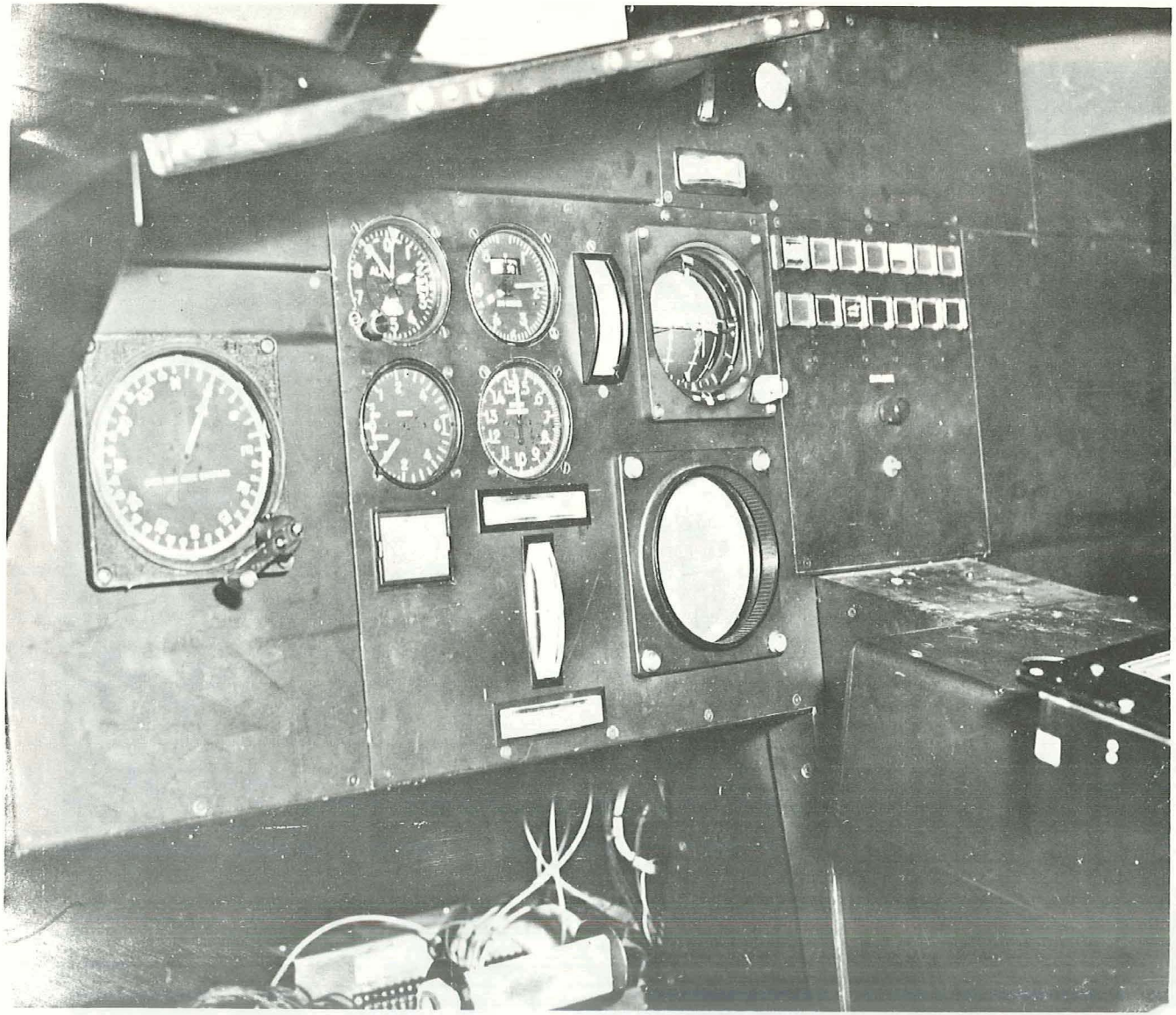

FIGURE 18: COCKPIT INTERIOR

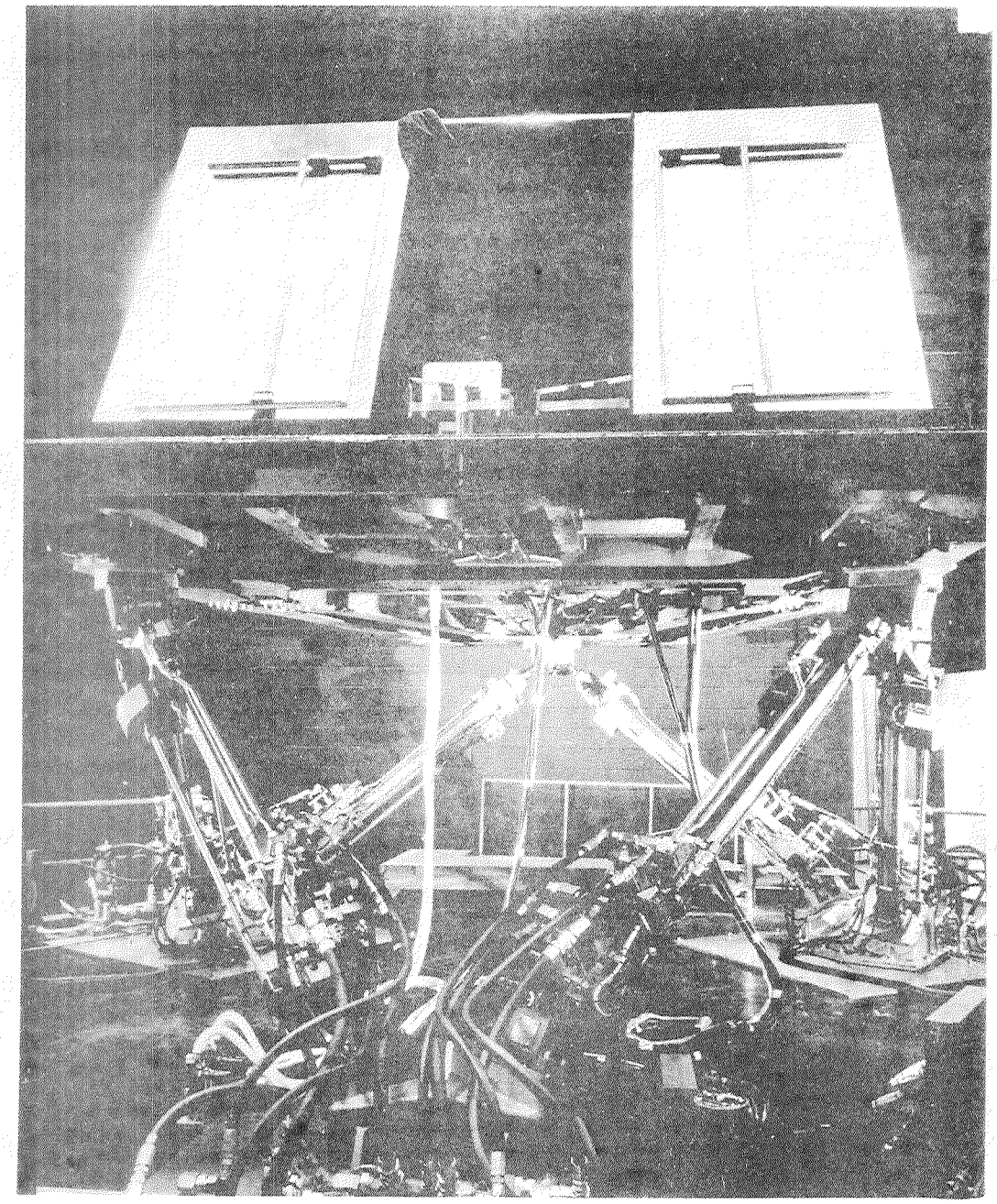

FIGURE 19: MOVING BASE SIMULATOR

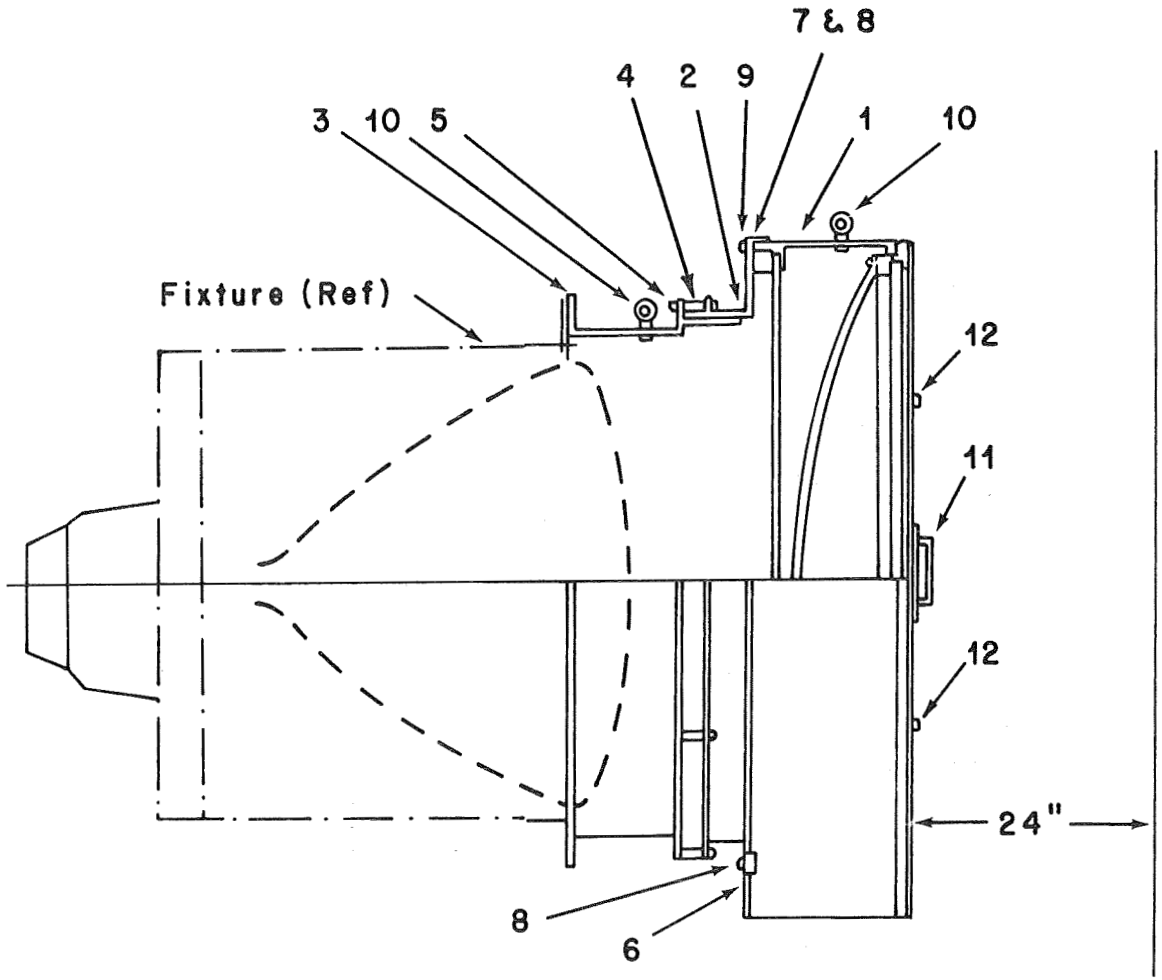

LEGEND

1. Window Assembly
2. Window Adapter
3. Frame Adapter
4. Spacer
5. Screw
6. Side Cover
7. Access Cover
8. Screw
9. Screw
10. Eyebolt
11. Front Cover
12. Plastic Fasteners

FIGURE 20: INFINITY DISPLAY OPTICAL ASSEMBLY
(PANCAKE WINDOW)

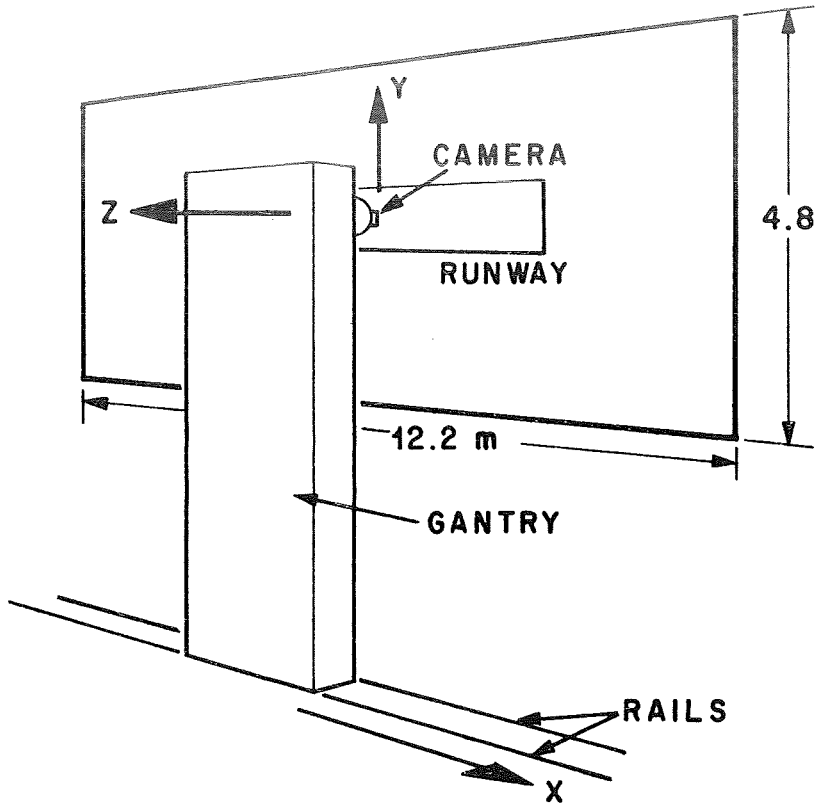

KSC AIRPORT AND SURROUNDING AREA

2500 - 1 SCALE (MAXIMUM ALTITUDE 1584.96 m)

CAMERA - BLACK AND WHITE, COLOR LATER

FIGURE 21: DALTO DISPLAY

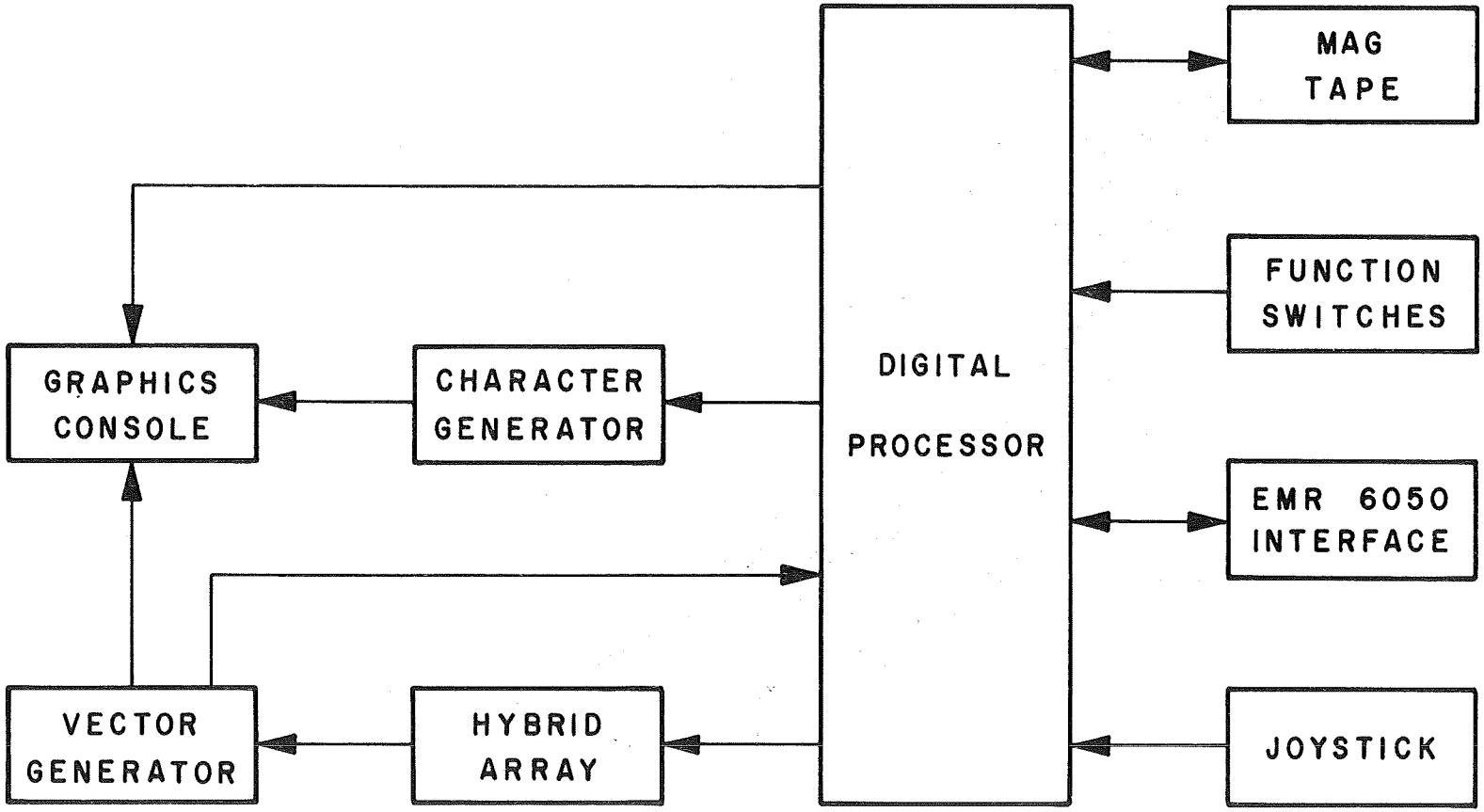

FIGURE 22: ADAGE GRAPHICS TERMINAL

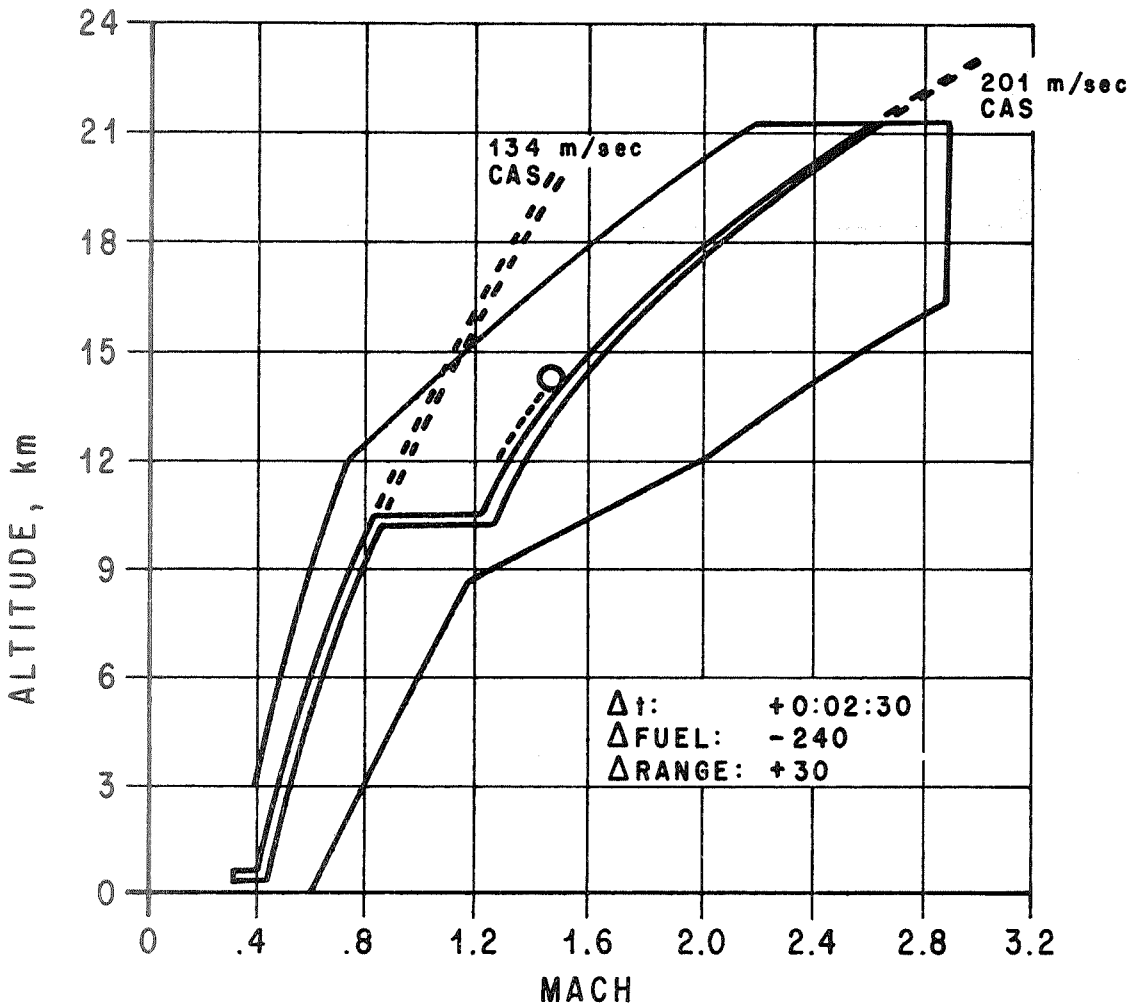

FIGURE 23: DESCENT

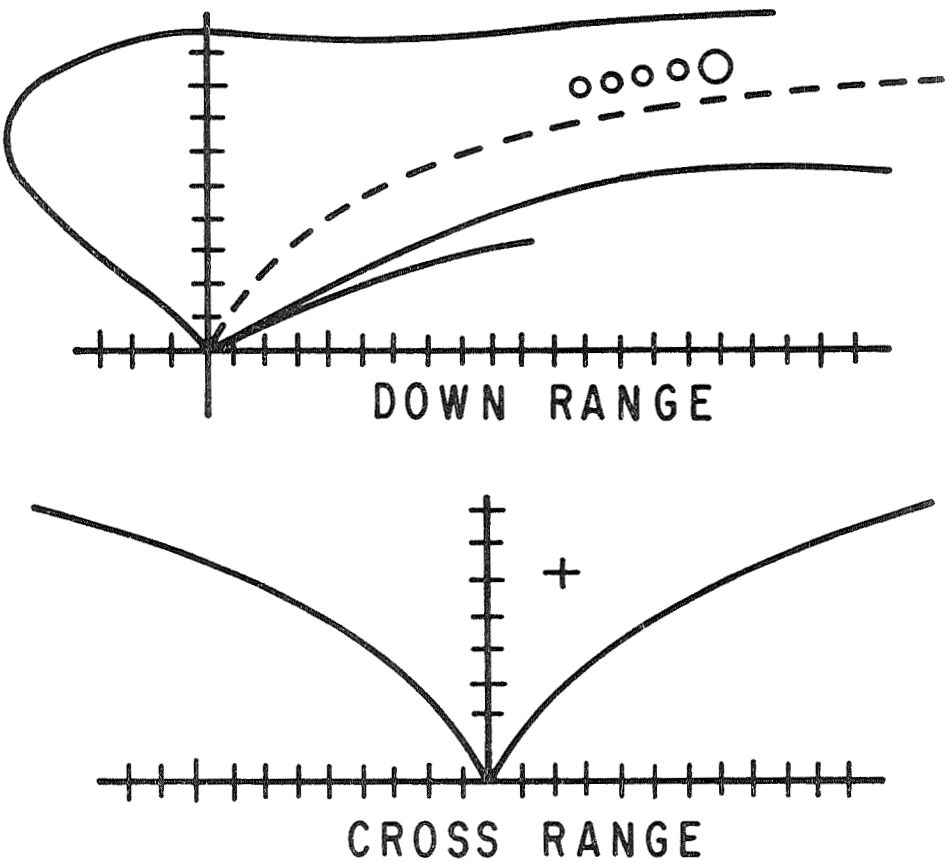

FIGURE 24: CROSS-RANGE AND DOWN-RANGE LANDING CORRIDORS

APPENDIX

ANALOG DIAGRAM OF SIMULATION

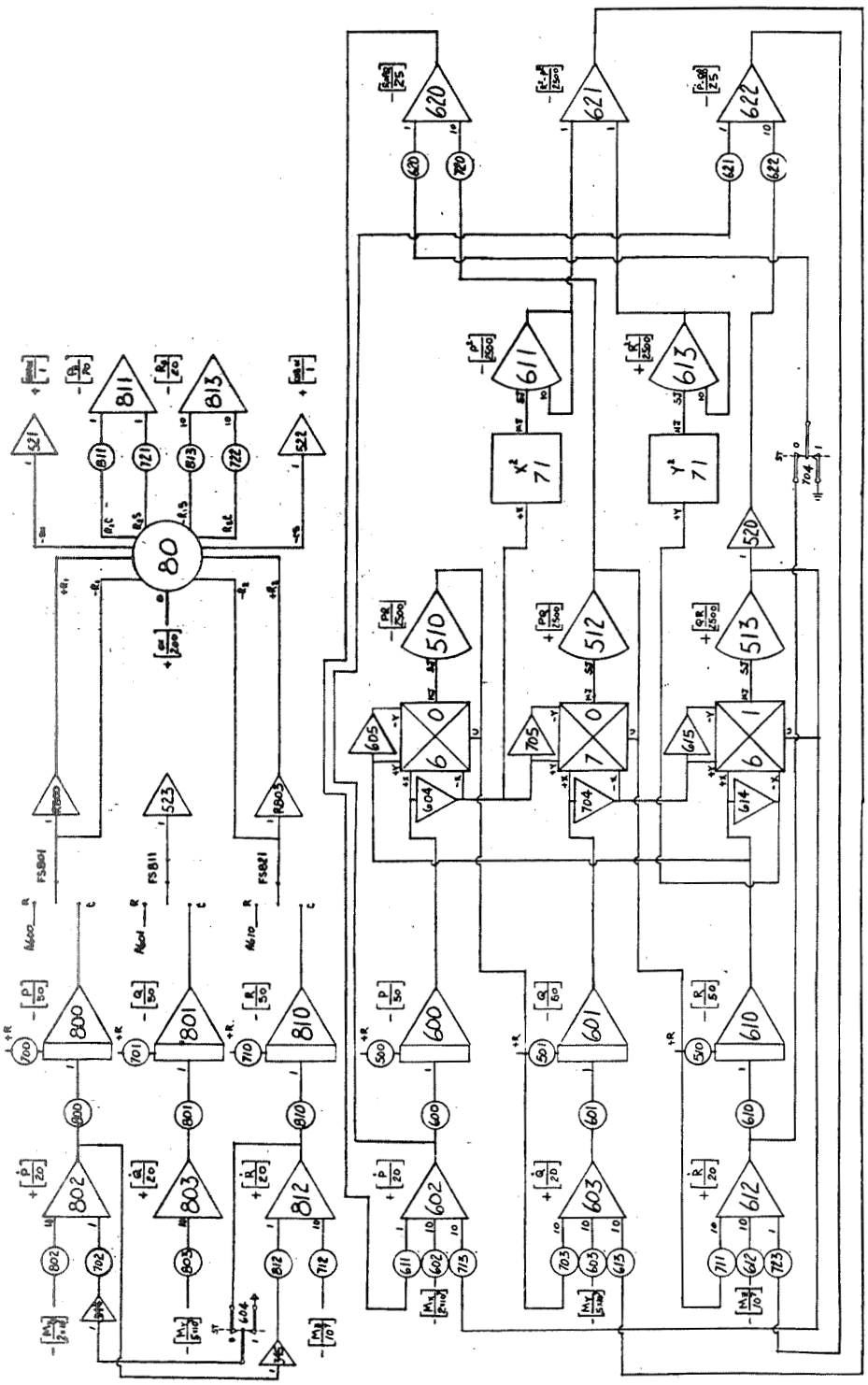

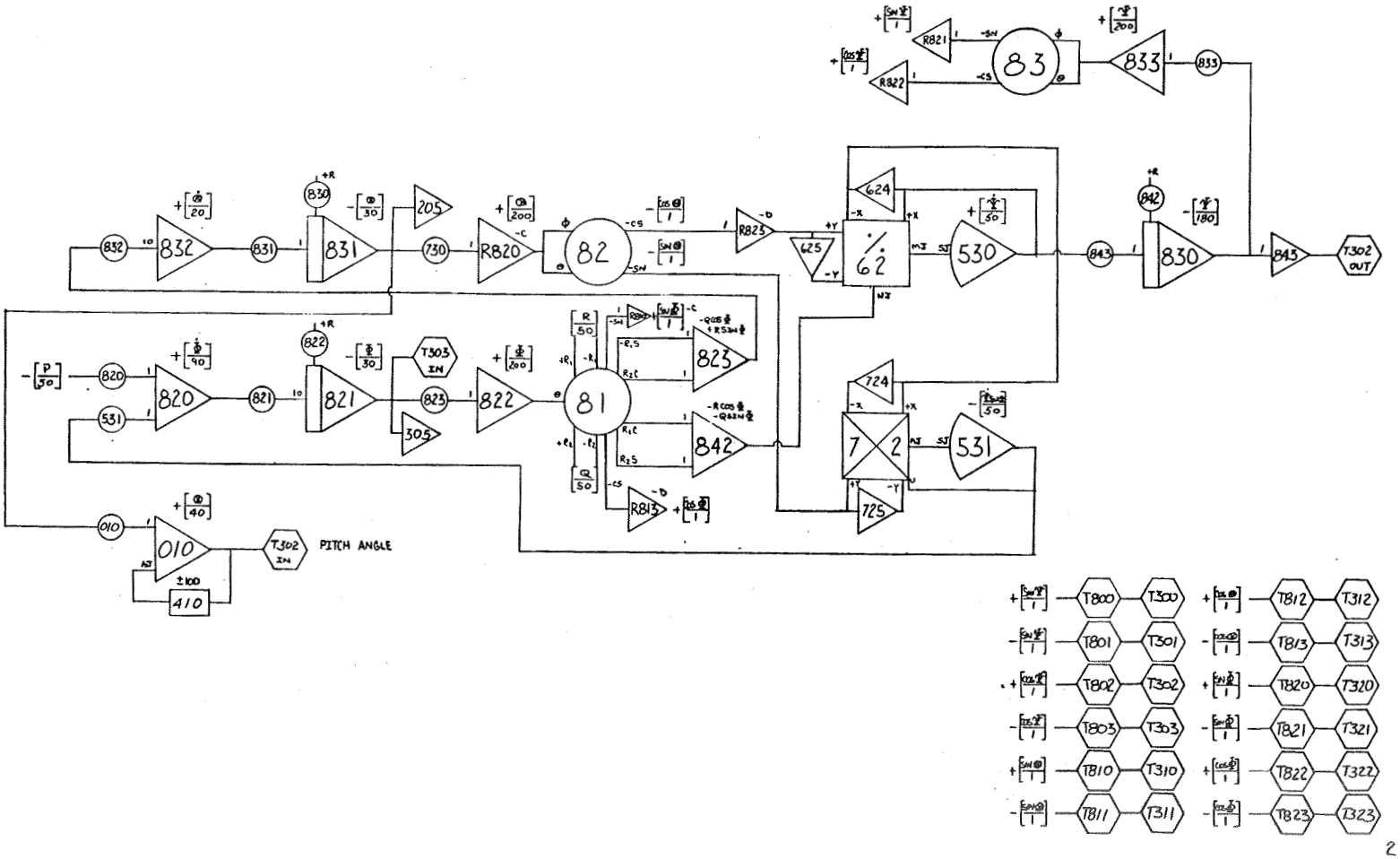
83
R821
R822
833
832
831
830
205
730
R820
82
R823
624
625
62
530
842
830
843
T302 OUT
820
821
822
823
305
T303 IN
81
823
842
R813
724
725
7
2
531
010
410
T302 IN
PITCH ANGLE
T800
T300
T801
T301
T802
T302
T803
T303
T810
T310
T811
T311
T812
T312
T813
T313
T820
T320
T821
T321
T822
T322
T823
T323

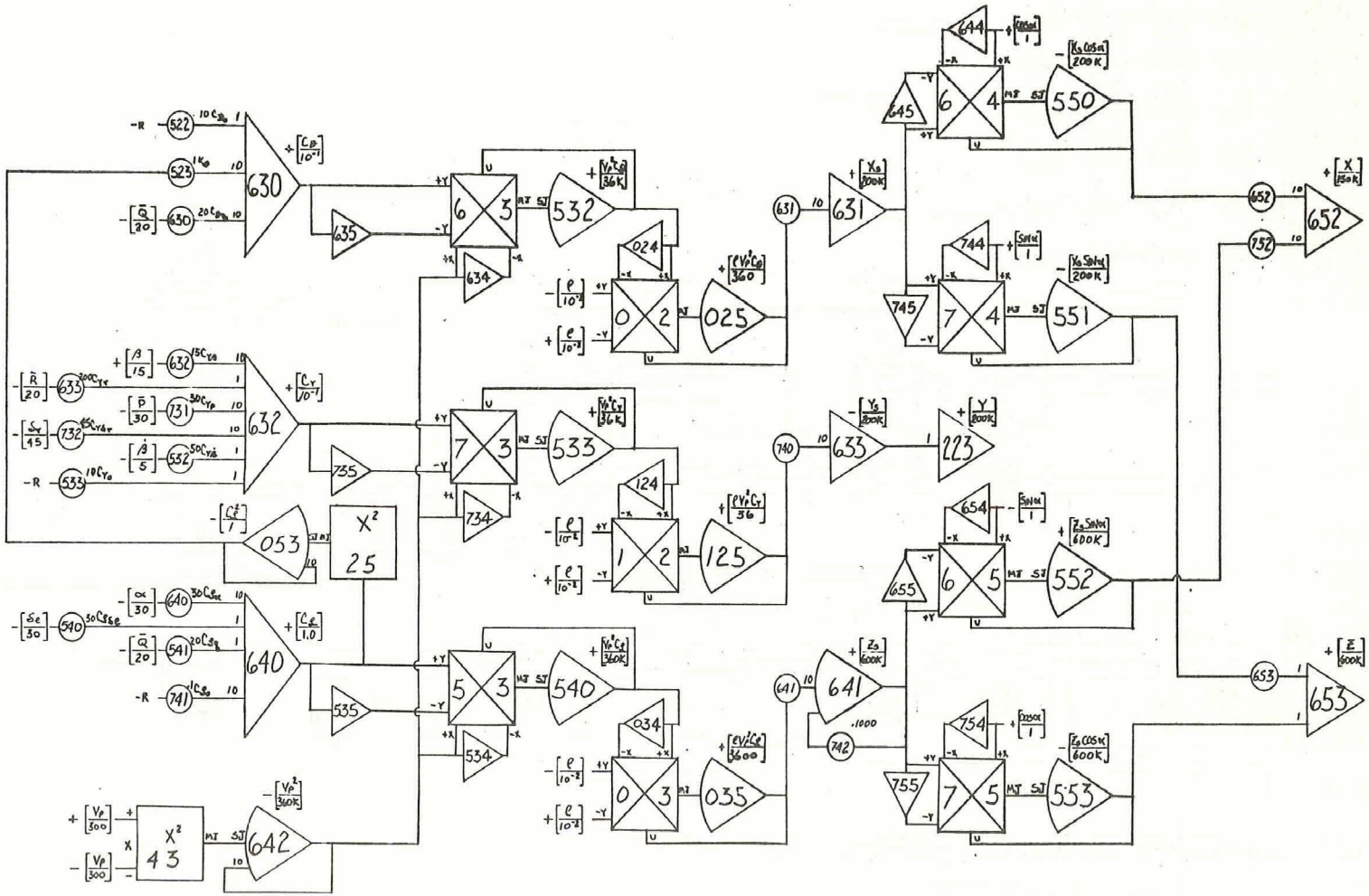

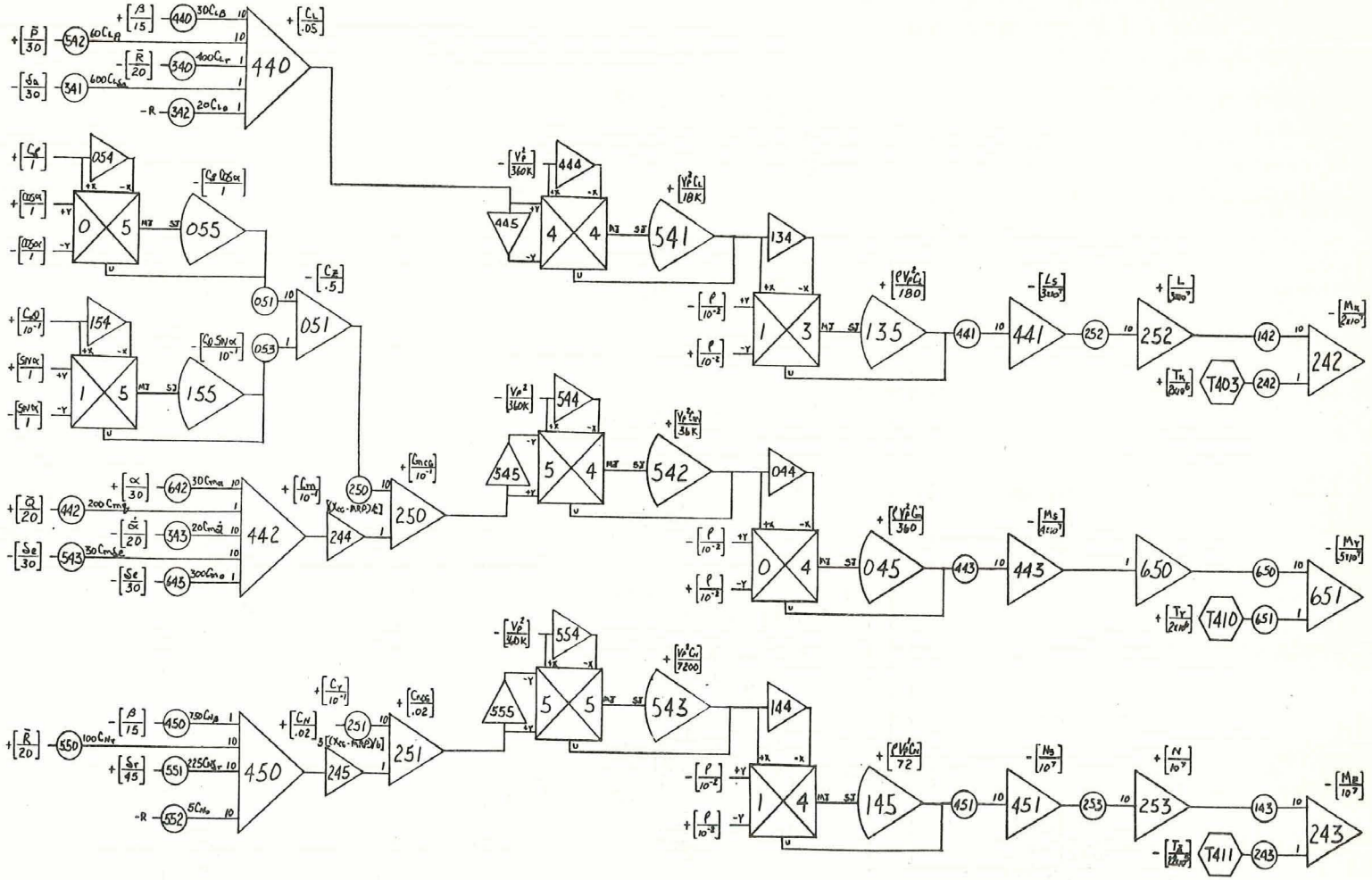

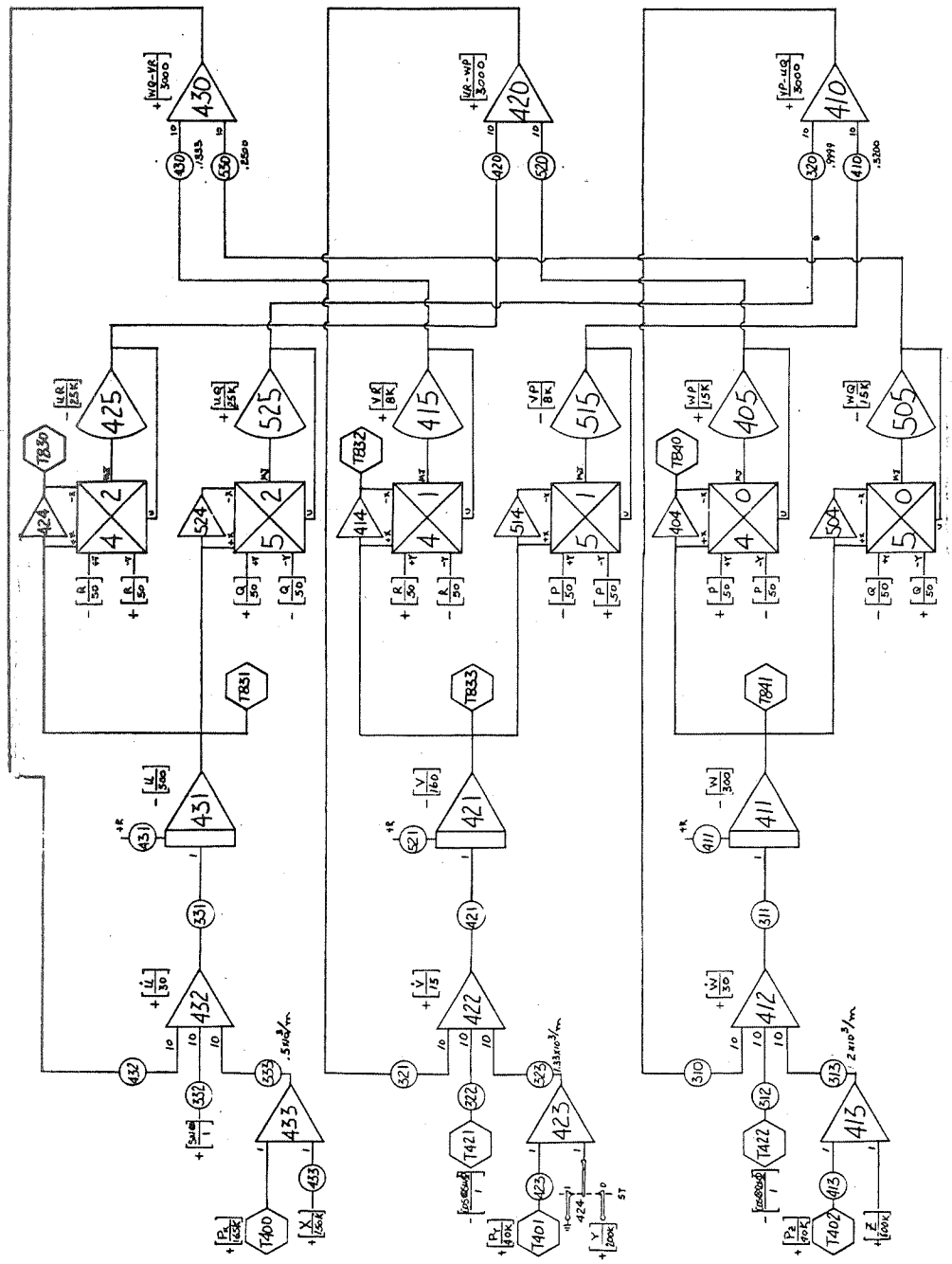

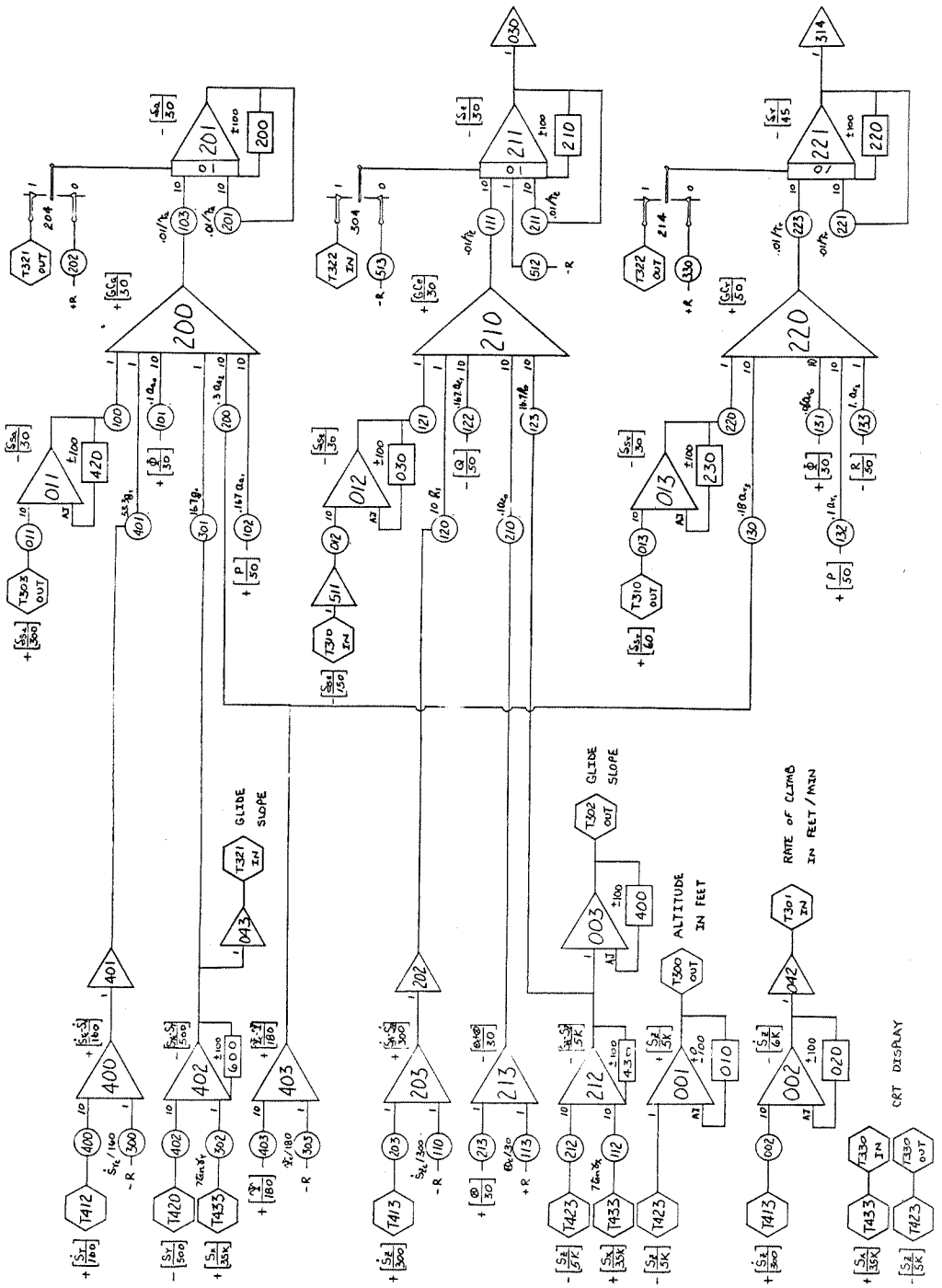
GLIDE SLOPE
ALTITUDE IN FEET
RATE OF CLIMB IN FEET / MIN
CRT DISPLAY

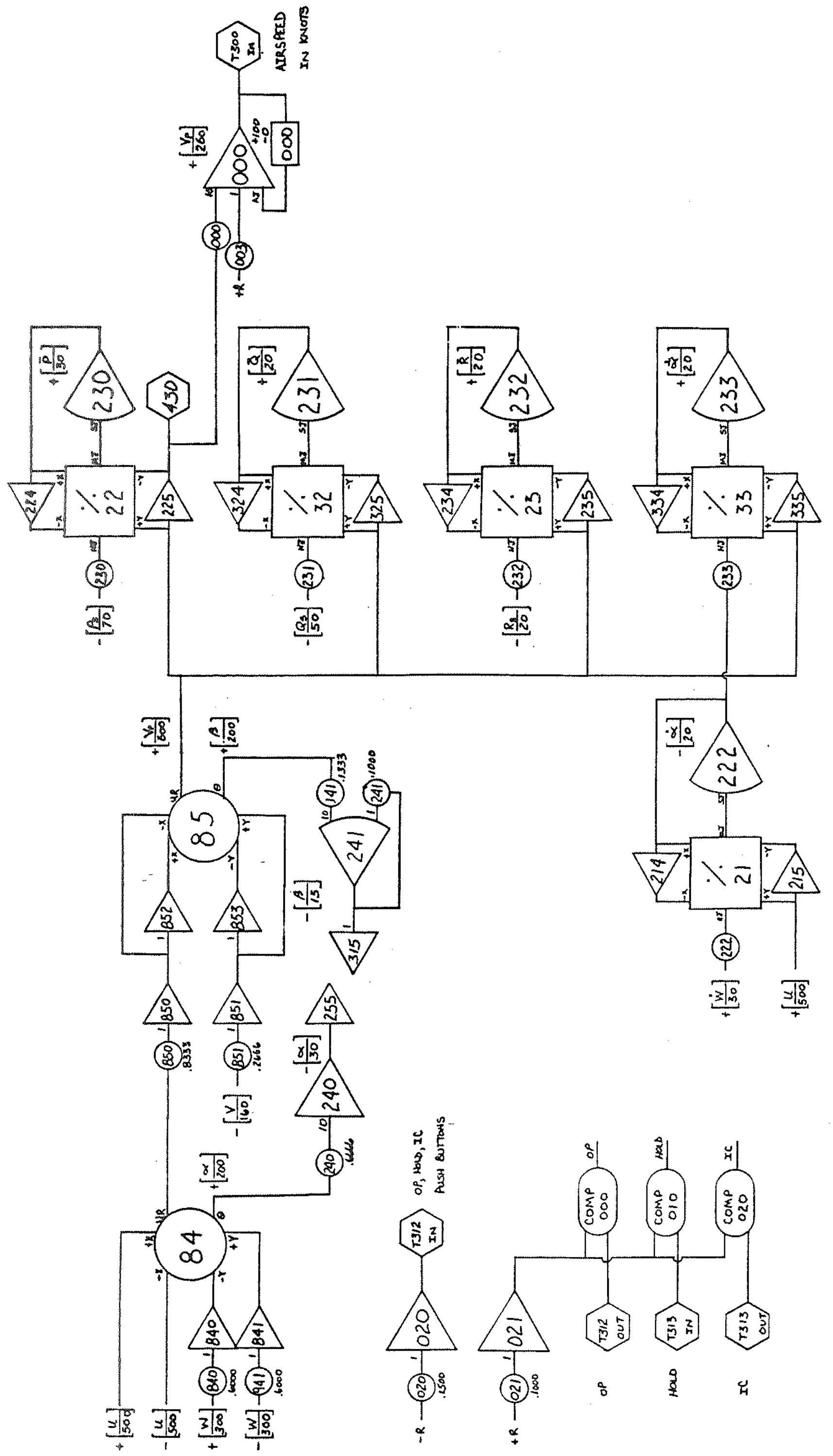
AIRSPEED IN KNOTS
OP, HOLD, IC PUSH BUTTONS
OP
HOLD
IC

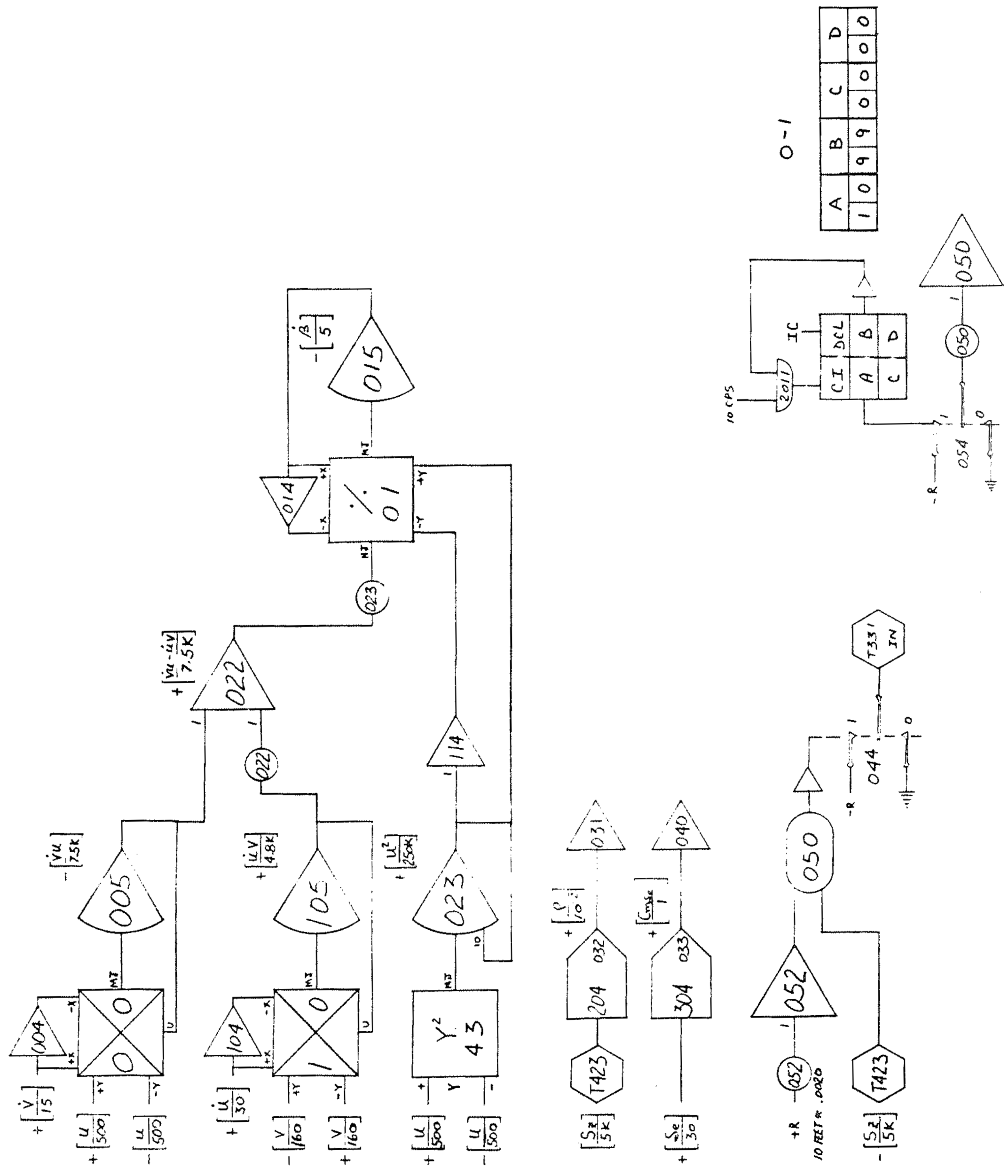
004
005
104
105
023
022
114
014
015
050
052
T423
T331 IN
044
054
2011
O-1

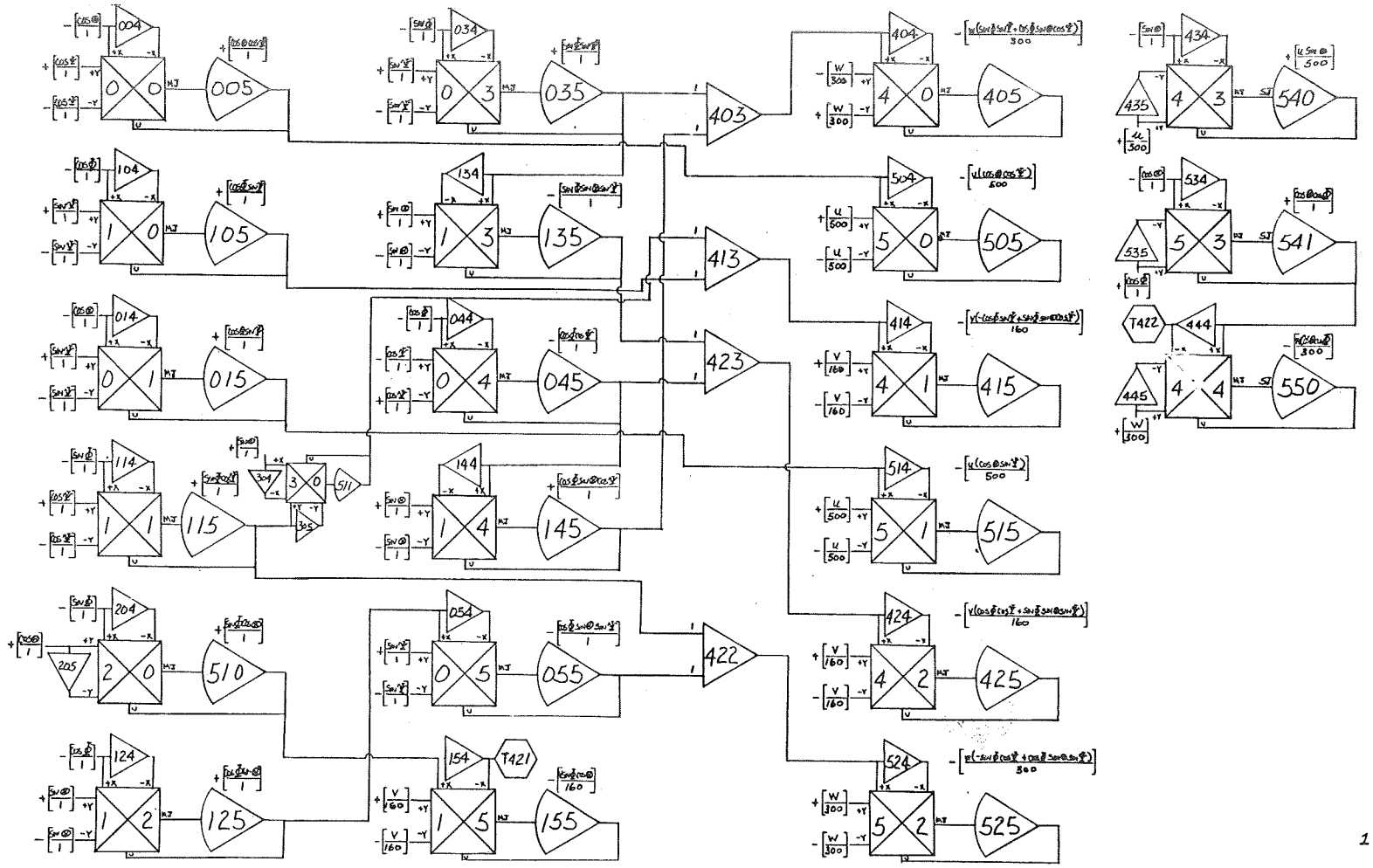

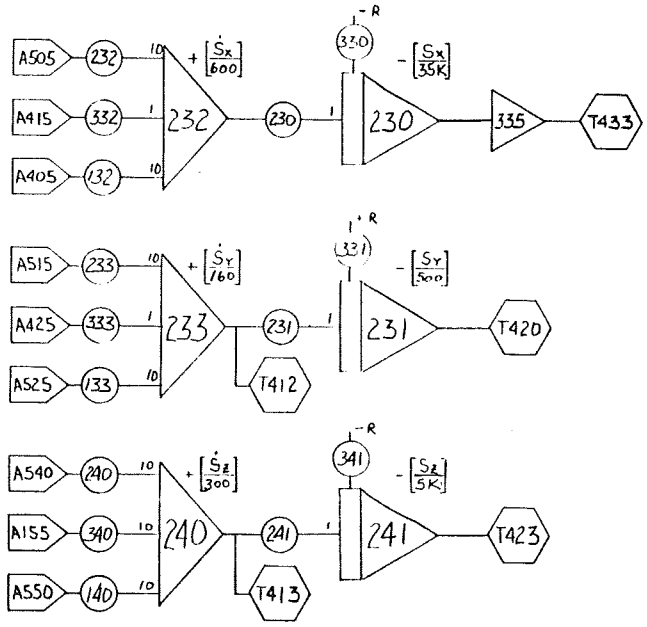
A505
232
10
+ [Ṡx / 600]
A415
332
1
232
A405
132
10
230
1
- R
330
1
- [Sx / 35K]
230
335
T433
A515
233
10
+ [Ṡy / 160]
A425
333
1
233
A525
133
10
231
T412
1
+ R
331
1
- [Sy / 500]
231
T420
A540
240
10
+ [Ṡz / 300]
A155
340
10
240
A550
140
10
241
T413
- R
341
1
- [Sz / 5K]
241
T423

3

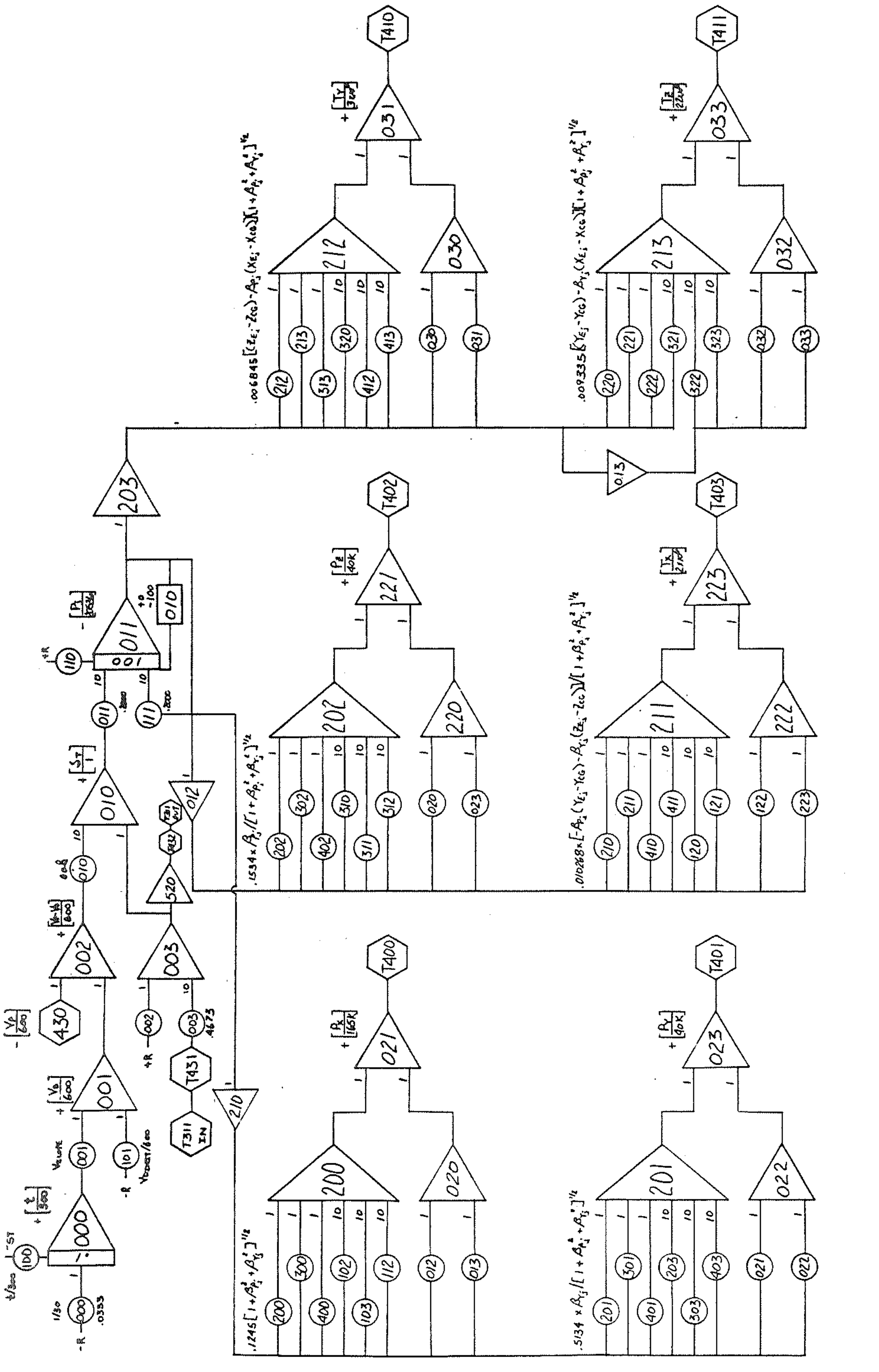
T410
T411
T402
T403
T400
T401
T431
T311 IN
031
033
030
032
212
213
221
223
202
211
220
222
200
201
021
023
020
022
203
013
011
010
012
520
210
000
001
002
003
430

APPROVAL

SHUTTLE SIMULATION

by Alberta King and Maurice Knighton

The information in this report has been reviewed for security classification. Review of any information concerning Department of Defense or Atomic Energy Commission programs has been made by the MSFC Security Classification Officer. This report, in its entirety, has been determined to be unclassified.

This document has also been reviewed and approved for technical accuracy.

D. K. Mower
Chief, Control Requirements Section

R. S. Ryan
Chief, Flight Analysis Branch

J. A. Lovingood
Chief, Dynamics and Control Division

E. D. Geissler
Director, Aero-Astrodynamics Laboratory

CONCURRENCE:

W. K. Polstorff
Chief, Simulation Branch

H. Hoelzer
Director, Computation Laboratory

DISTRIBUTION

DIR
DEP-T
A&TS-PAT
PM-PR-M, Mr. Goldston
A&TS-MS-H
A&TS-MS-IP
A&TS-MS-IL (8)
A&TS-TU, Mr. Wiggins (6)

S&E-ASTR
Mr. Moore
Mr. Scofield
Mr. Mink
Mr. Brooks

S&E-ASTN
Mr. Heimburg
Mr. Hoodless
Mr. Thompson

S&E-CSE
Dr. Haeussermann
Mr. Blackstone
Mr. Mack
Mr. Hammers
Mr. Gregory
Mr. Grote
Mr. Green
Mr. Jean, -T

PD
Mr. Godfrey
Mr. Odom
Mr. Sumrall
Mr. Weaver

S&E-COMP
Dr. Hoelzer
Dr. Polstorff
Mr. Knighton (10)

S&E-AERO
Dr. Geissler
Mr. Horn
Dr. Lovingood
Mr. Lindberg
Mr. Baker
Mr. W. Vaughan
Mr. Blair
Dr. Fichtl
Mr. Dahm
Mr. Bacchus
Mr. Dunn
Mr. Ryan (10)
Mr. Mowery
Mr. Hall
Mr. Livingston
Mr. McAnnally
Mr. Sims
Mr. Elrod
Mr. Nunley
Mrs. King (10)
Mr. Lofton
Mrs. Hightower

Sci. & Tech. Info. Facility (25)
P. O. Box 33
College Park, Md. 20740
Attn: NASA Rep. (S-AK/RKT)

Manned Spacecraft Center
Houston, Texas
Attn: Mr. Kennedy, Code EG13
G&C Adv. Studies, Bldg. 16
Don Cheatam

MSFC—RSA, Ala